Expression profiling of uterine leiomyomata cytogenetic subgroups reveals distinct signatures in matched myometrium: transcriptional profiling of the t(12;14) and evidence in support of predisposing genetic heterogeneity

Jennelle C. Hodge[1,3,4], Tae-Min Kim[3], Jonathan M. Dreyfuss[6], Priya Somasundaram[1], Nicole C. Christacos[1,3,8], Marissa Rousselle[1], Bradley J. Quade[2,3], Peter J. Park[3,6,7], Elizabeth A. Stewart[1,3,5] and Cynthia C. Morton[1,2,3,6,*]

[1]Department of Obstetrics, Gynecology and Reproductive Biology and [2]Department of Pathology, Brigham and Women's Hospital, Boston, MA 02115, USA, [3]Harvard Medical School, Boston, MA 02115, USA, [4]Department of Laboratory Medicine and Pathology and [5]Department of Obstetrics and Gynecology, Mayo Clinic, Rochester, MN 55905, USA, [6]Harvard-Partners Center for Genetics and Genomics, Boston, MA 02115, USA, [7]Children's Hospital Informatics Program, Boston, MA 02115, USA and [8]Cytogenetics Department, Quest Diagnostics Nichols Institute, Chantilly, VA 20151, USA

Uterine leiomyomata (UL), the most common neoplasm in reproductive-age women, are classified into distinct genetic subgroups based on recurrent chromosome abnormalities. To develop a molecular signature of UL with t(12;14)(q14-q15;q23-q24), we took advantage of the multiple UL arising as independent clonal lesions within a single uterus. We compared genome-wide expression levels of t(12;14) UL to non-t(12;14) UL from each of nine women in a paired analysis, with each sample weighted for the percentage of t(12;14) cells to adjust for mosaicism with normal cells. This resulted in a transcriptional profile that confirmed *HMGA2*, known to be overexpressed in t(12;14) UL, as the most significantly altered gene. Pathway analysis of the differentially expressed genes showed significant association with cell proliferation, particularly G1/S checkpoint regulation. This is consistent with the known larger size of t(12;14) UL relative to karyotypically normal UL or to UL in the deletion 7q22 subgroup. Unsupervised hierarchical clustering demonstrated that patient variability is relatively dominant to the distinction of t(12;14) UL compared with non-t(12;14) UL or of t(12;14) UL compared with del(7q) UL. The paired design we employed is therefore important to produce an accurate t(12;14) UL-specific gene list by removing the confounding effects of genotype and environment. Interestingly, myometrium not only clustered away from the tumors, but generally separated based on associated t(12;14) versus del(7q) status. Nine genes were identified whose expression can distinguish the myometrium origin. This suggests an underlying constitutional genetic predisposition to these somatic changes which could potentially lead to improved personalized management and treatment.

*To whom correspondence should be addressed at: Harvard Medical School, 77 Avenue Louis Pasteur, New Research Building Room 160, Boston, MA 02115, USA. Tel: +1 6175254535; Fax: +1 6175254533; Email: cmorton@partners.org

INTRODUCTION

Benign smooth muscle tumors of the uterus generally referred to as fibroids are the most common neoplasm of the female genital tract, occurring in up to 77% of women as defined by serial sectioning of uteri (1). These uterine leiomyomata (UL) are clinically detectable in 25% of reproductive-age women, many of whom have significant morbidity often necessitating surgery to alleviate excessive menstrual bleeding, pelvic pain, urinary complaints, constipation and reproductive dysfunction (2–4). UL are therefore the primary indication for hysterectomy, the cause for approximately one in five visits to a gynecologist, and result in expenditures exceeding 2.1 billion health-care dollars annually in the USA (5–7).

Molecular pathways underlying UL development and growth acceleration are largely unknown and most recent discoveries have stemmed from studying recurrent cytogenetic abnormalities identified among the ∼40% of karyotypically abnormal UL (8,9). One of the most common subgroups is characterized by rearrangement of 12q14-15, typically as a t(12;14)(q14-15;q23-24), which occurs in ∼7.5% of all UL and 20% of karyotypically abnormal UL (10). This high prevalence of t(12;14) and its frequent occurrence as the sole cytologically detectable chromosome abnormality suggest a primary importance for this translocation in UL tumorigenesis.

The presence of t(12;14) has been associated with larger sized UL than those with either normal karyotypes or interstitial 7q22 deletions (11–13). In particular, a systematic study of every palpable UL in each of 96 women undergoing hysterectomy without pretreatment removed any potential bias in determining significance due to tumor sampling (i.e. selection of only larger tumors mainly as a result of myomectomy rather than hysterectomy) or due to pretreatment with gonadotropin-releasing hormone-agonists that can be used to shrink tumors prior to surgery (11).

UL with t(12;14) have elevated expression of the high mobility group (HMGA) family member *HMGA2* located at 12q14.3 (14,15). This architectural factor is a non-histone component of chromatin that alters DNA conformation to modulate access of transcription factors to their target genes, thereby influencing differentiation and proliferation of mesenchymal tissues (16–19). Consistently, transgenic mice null for *Hmga2* have a 40% reduction in weight known as the *pygmy* phenotype (20,21). In fact, *HMGA2* expression in both mice and humans is mainly restricted to proliferating embryonic tissues, predominantly mesenchymal derivatives including the myometrium from which UL arise, and are notably absent from differentiated adult non-proliferating counterparts (15,22,23). In addition, phosphorylation of *HMGA* proteins by cdc2 kinase modulates their DNA binding ability in a cell cycle-dependent manner (24). This role of *HMGA2* in growth was recently extended to include an association with human height (25,26), which is further illustrated by an intragenic rearrangement in *HMGA2* from a constitutional chromosome 12 inversion resulting in extreme multisystem overgrowth identified in the Guinness Book of World Records tallest teenager record holder (27). In contrast to such *in vivo* analyses, tissue culture induction of *HMGA2* expression has been shown in a variety of human tissues including myometrium and karyotypically normal UL (15), attributed to a serum component or the weak estrogenic effect of phenol red in culture media (28). This confounds the use of *in vitro* methods and necessitates direct examination of gene expression in UL tumors.

UL provide a unique *in vivo* model as on average six to seven independent clonal tumors occur per woman. The clonal nature of UL was confirmed by the presence of t(12;14) UL in the same uterus as UL harboring different or no chromosomal changes (1), as well as by analysis of repeat polymorphisms in the X-linked androgen receptor and phosphoglycerokinase genes (29–31). We have taken advantage of these circumstances for expression profiling to compare directly UL with t(12;14) to UL without t(12;14) obtained concurrently from the same uterus.

We demonstrate that such a matched (or paired) study design is a requisite to identify the molecular profile associated with the t(12;14) subgroup. This design, previously validated for the interstitial 7q22 deletion UL subgroup (32), has not been exploited by any prior study of t(12;14) in UL. Importantly, it obviates the confounding effects of patient-to-patient variability due to divergent genotype, environment or genotype/environment interaction. In addition, the unique expression profiles we identify for myometrial samples from women with t(12;14) UL relative to those with del(7q) UL suggest an underlying genetic predisposition to these somatic alterations.

RESULTS

Screening for t(12;14) UL by fluorescence *in situ* hybridization and karyotyping

To identify UL with t(12;14), interphase fluorescence *in situ* hybridization (FISH) or karyotype analysis was employed (Table 1). A conservative false-positive cut-off of 15% for t(12;14) interphase FISH was established by doubling the positive rate found in normal peripheral blood lymphocytes. Probe binding to the correct target region without cross-hybridization was validated on lymphocyte metaphases. Screening of 348 tumors from 140 patients identified 35 t(12;14) UL (10%). Of these 35 UL, those with matched myometrium and non-t(12;14) samples, as well as a single case found through karyotyping that was confirmed by FISH, were selected for further analysis resulting in a total of nine cases. In these t(12;14) UL, the level of mosaicism of cells not carrying the abnormality ranged from 0 to 84%. Case 3 also had a proportion of cells (25%) with another recurrent UL karyotypic abnormality, interstitial deletion of 7q22.

Identification of t(12;14)-specific UL genes

RNA from each t(12;14) UL as well as from concurrently collected non-t(12;14) UL and normal myometrium tissues from each of nine cases was hybridized on Affymetrix GeneChip Human Genome U133 Plus 2.0 oligonucleotide arrays for expression analysis. Among these cases, multiple clinical features were variable such as UL size, patient age, race and stage of menstrual cycle at the time of surgical removal (Table 2). To control for such variables, a direct comparison

Table 1. Histopathology, karyotype and FISH results of UL

Case number	Accession number	Sample type	Histopathology	Karyotype	% t(12;14)	Gene Expression Omnibus (GEO) identifier[a]
1	ST99-240	t(12;14) UL	Usual type, low MI	46,XX,t(12;14) (q15;q23-24)[10]	100[c]	GSM452325
	ST99-241	Non-t(12;14) UL	Usual type, low MI	46,XX[12]	0[c]	GSM452324
	ST99-243	Myometrium	—[b]	—	—	GSM452323
2	ST04-041	t(12;14) UL	—	—	30[d]	GSM452328
	ST04-043	Non-t(12;14) UL	—	—	0[d,e]	GSM452327
	ST04-045	Myometrium	—	—	—	GSM452326
3[f]	ST04-065	t(12;14) UL	—	—	25% del(7q)/16% t(12;14)[d]	GSM452331
	ST04-066	Non-t(12;14) UL	—	—	1% del(7q)/7% t(12;14)[d,e]	GSM452330
	ST04-067	Myometrium	—	—	—	GSM452329
4	ST04-118F-2	t(12;14) UL	Usual type, low MI	—	100[d]	GSM452334
	ST04-118F-1	Non-t(12;14) UL	Usual type, low MI	—	4[d,e]	GSM452333
	ST04-118M	Myometrium	Normal myometrium	—	—	GSM452332
5	ST05-019F-1	t(12;14) UL	Mildly cellular, low MI	—	48[d]	GSM452337
	ST05-019F-2	Non-t(12;14) UL	Mildly cellular, low MI	—	0[d,e]	GSM452336
	ST05-019M	Myometrium	—	—	—	GSM452335
6[g]	ST05-024F-4	t(12;14) UL	Usual type, low MI	—	30[d]	GSM452341
	ST05-024F-5	Non-t(12;14) UL	Usual type, low MI	—	5[d,e]	GSM452340
	ST05-024M	Myometrium	—	—	—	GSM452339
7	ST05-031F-1	t(12;14) UL	Usual type, low MI	—	63[d]	GSM452344
	ST05-031F-3	Non-t(12;14) UL	Usual type, low MI	—	3[d,e]	GSM452343
	ST05-031M	Myometrium	—	—	—	GSM452342
8	ST06-040F-1	t(12;14) UL	Usual type, low MI	—	77[d]	GSM452347
	ST06-040F-2	Non-t(12;14) UL	Usual type, low MI	—	8[d,e]	GSM452346
	ST06-040M	Myometrium	—	—	—	GSM452345
9	ST06-042F-5	t(12;14) UL	Usual type, low MI	—	83[d]	GSM452350
	ST06-042F-1	Non-t(12;14) UL	Usual type, low MI	—	4[d,e]	GSM452349
	ST06-042M	Myometrium	—	—	—	GSM452348

[a]http://www.ncbi.nlm.nih.gov/geo/.
[b]Dash indicates unknown.
[c]Percentage of t(12;14) cells determined by karyotype.
[d]Percentage of t(12;14) cells determined by FISH.
[e]Value below FISH false-positive cut-off for t(12;14) of 15%.
[f]Case 3 is a mosaic del(7q)(q22q32)/t(12;14)(q15;q23-q24) UL also reported as Case 5 in Hodge *et al.* (32).
[g]Case 6 has an independent del(7q) UL which is reported as Case 10 in Hodge *et al.* (32).

Table 2. Clinical features of UL

Case number	Size of t(12;14) tumor (cm)	Size of non-t(12;14) tumor (cm)	Total number of tumors	Race	Age of onset (years)[a]	Age at surgery (years)	Menstrual cycle[b]
1	11.5	14.7	3	White	47	47	Proliferative
2	—[c]	—	4	White	56	57	Menopausal
3	—	—	3	White	40	43	Menstruation
4	9.5 × 7.5 × 7	2.5 × 1.9 × 1.4	8	Asian	38	42	Artificial menopause (gonadotropin-releasing hormone-agonist pretreatment)
5	10 × 8.9 × 8.4	2.8 × 2.4 × 2.2	3	White	49	49	Secretory
6	5 × 4.5 × 4.5	5 × 4 × 4	10	White	51	59	Menopausal
7	18.5 × 12.5 × 10.5	4.5 × 4 × 3.6	5	White	41	51	Menopausal
8	15 × 13 × 13	1.5 × 1.5 × 1.5	4	White	36	46	Secretory
9	4 × 4 × 2.5	11 × 6 × 5.5	12	Asian	35	36	Secretory

[a]Self-reported by patient.
[b]Based on day 1 of last menstrual period relative to surgery date (days 1–5 = menstruation; 6–14 = proliferative; 14–28+ = secretory; >100 days = menopausal).
[c]Dash indicates unknown.

of the array expression data was made between tissues obtained from each individual to identify differences in expression specifically resulting from the t(12;14). A heatmap from an unsupervised hierarchical cluster analysis of the 500 most variable genes demonstrates a tendency of myometrium tissues to cluster separately from UL samples and for the
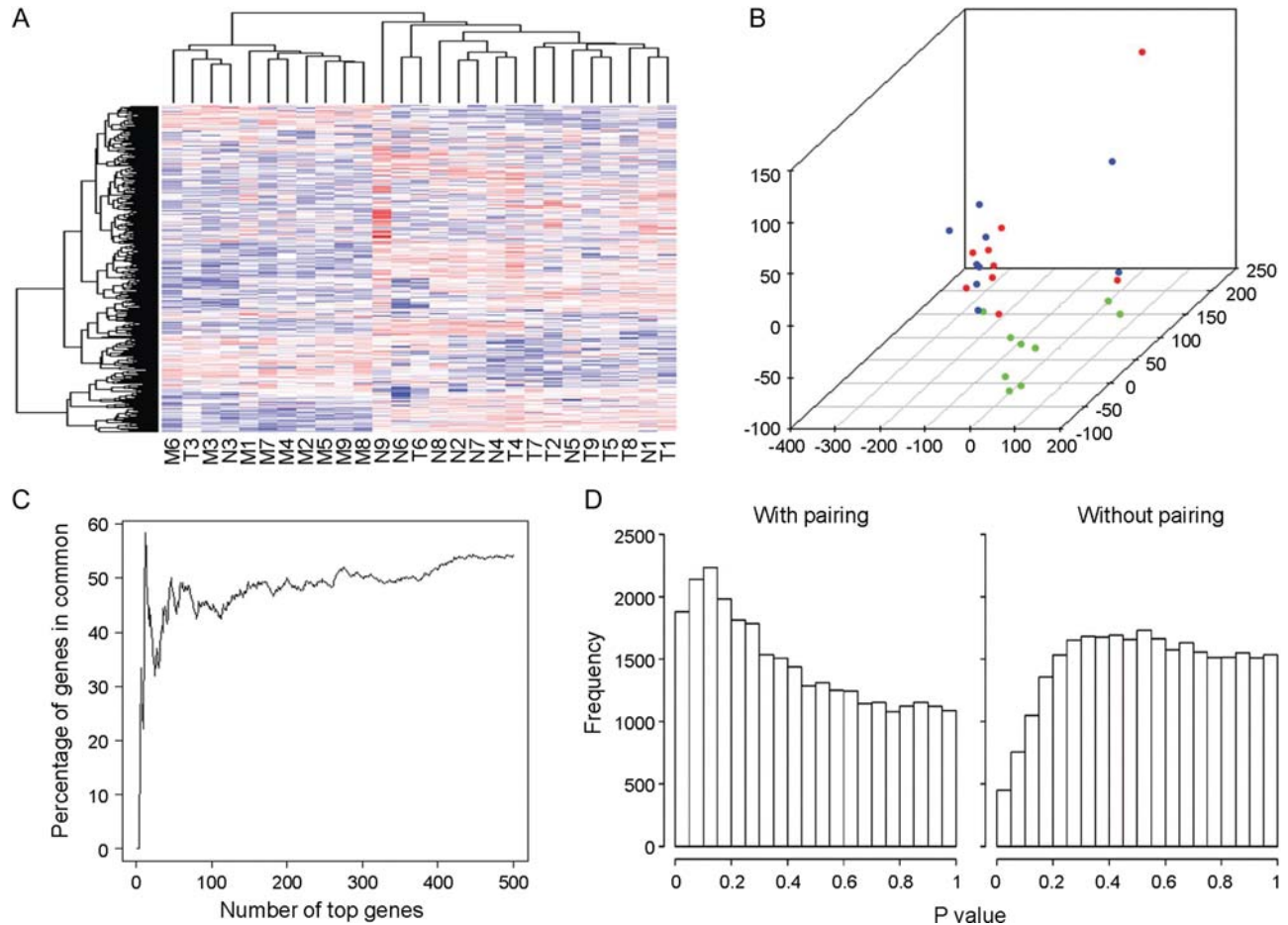
Figure 1. Paired analysis of the t(12;14) UL and non-t(12;14) UL microarray data to control for patient-to-patient variability without involvement of the myometrium is necessary to generate an accurate t(12;14) UL-specific gene list. (**A**) A heatmap of an unsupervised hierarchical cluster analysis of the 500 most variable genes between myometrium (M), t(12;14) UL (T) and non-t(12;14) UL (N) from each of the nine women shows a trend of myometrial separation from all UL tissues and of UL clustering based on patient rather than t(12;14) status. A similar result is obtained when more genes are included in the analysis. (**B**) Unsupervised principal component analysis displays in three dimensions the tendency of the myometrial samples (green) to cluster and have only minimal overlap with the t(12;14) (blue) and non-t(12;14) UL tissues (red). (**C**) A comparison of the percent of genes in common between a paired and unpaired analysis of t(12;14) UL versus non-t(12;14) UL indicates that the two modes of analysis produce different gene lists. (**D**) The distribution of *P*-values for two-group comparison *t*-tests using a paired analysis includes a peak on the left side, indicating that more genes were found with significant *P*-values than expected in a random data set. In contrast, the unpaired analysis generates a decreased or nearly flat distribution, suggesting that genes with significant *P*-values identified by such an assessment are not likely to be true positives.

t(12;14) UL and non-t(12;14) UL to cluster by patient rather than by presence or absence of the translocation (Fig. 1A). Separation of the myometrial samples from the overlapping UL groups can be visualized in three dimensions through principal component analysis (Fig. 1B). These results suggest that incorporation of the myometrial array data is suited to determining genes that differentiate any UL from the normal myometrial tissue rather than identifying the t(12;14)-specific UL genes. Therefore, myometrial samples were not included in further analyses of t(12;14)-specific genes.

The importance of controlling for patient-to-patient variability is illustrated by comparing the percent of genes overlapping between gene lists generated by a paired and an unpaired analysis of the t(12;14) UL and non-t(12;14) UL expression data. The two analyses had an ∼50% gene overlap (Fig. 1C). Another demonstration of the need to account for variability between patients is shown by examining the distribution of *P*-values from paired and unpaired *t*-tests for a

two-group comparison (Fig. 1D). In the paired case, which considers the difference between samples of the same individual, the resultant peak on the left side of the distribution indicates that more genes with significant *P*-values were identified than expected from a random data set. In contrast, the unpaired analysis ignores the sample pairing and results in a distribution showing no clear evidence that genes appearing to have significant *P*-values from such a study design would be true positives. Based on these analyses, paired *t*-tests directly contrasting the t(12;14) UL and the non-t(12;14) UL from each individual were chosen to determine t(12;14)-associated genes. This resulted in a list of genes ordered by their genome-wide significance levels corrected for multiple testing by the false discovery rate (*Q*-value) (33). Of the 100 most significant t(12;14) UL-specific genes, those with decreased expression are reported in Table 3 and those with increased expression in Table 4. A more extensive data set of 300 genes is provided as Supplementary Material, Table S1.

Table 3. Genes down-regulated in t(12;14) UL compared with non-t(12;14) UL

Number[a]	Probe set	Ref. Seq.	Gene symbol	Gene title	Fold change	*P*-value	*Q*-value	Chromosome
2	225619_at	NM_001040153	SLAIN1	SLAIN motif family, member 1	−3.1	2.30E − 05	0.25	13q22.3
4	238018_at	NM_001002919	FAM150B	Family with sequence similarity 150, member B	−4.2	0.00015	0.43	2p25.3
8	219290_x_at	NM_014395	DAPP1	Dual adaptor of phosphotyrosine and 3-phosphoinositides	−3.6	0.00024	0.43	4q23
10	222549_at	NM_021101	CLDN1	Claudin 1	−5.5	0.00027	0.43	3q28
13	241835_at	—[b]	—	CDNA clone IMAGE:4822225	−2.1	0.00036	0.43	1p36.13
20	211276_at	NM_080390	TCEAL2	Transcription elongation factor A (SII)-like 2	−4.9	0.00039	0.43	Xq22.1
34	229515_at	NM_002583	PAWR	PRKC, apoptosis, WT1, regulator	−1.8	0.00086	0.5	12q21.2
36	239381_at	NM_005046	KLK7	Kallikrein-related peptidase 7	−2.4	0.00092	0.5	19q13.33
38	204485_s_at	NM_005486	TOM1L1	Target of myb1 (chicken)-like 1	−2	0.001	0.5	17q22
44	204591_at	NM_006614	CHL1	Cell adhesion molecule with homology to L1CAM (close homolog of L1)	−3.2	0.0011	0.5	3p26.3
45	230353_at	—	LOC284112	Hypothetical protein LOC284112	−2.5	0.0011	0.5	17p13.2
51	213905_x_at	NM_001711	BGN	Biglycan	−1.8	0.0013	0.5	Xq28
57	226231_at	—	—	Transcribed locus	−3	0.0013	0.5	20q13.12// 12q21.2
61	226863_at	NM_001077710	FAM110C	Family with sequence similarity 110, member C	−2.4	0.0014	0.5	2p25.3
64	219737_s_at	NM_020403	PCDH9	Protocadherin 9	−2.8	0.0016	0.52	13q21.32
77	228155_at	NM_032333	C10orf58	Chromosome 10 open reading frame 58	−1.8	0.002	0.52	10q23.1
88	239153_at	—	FLJ41747	Hypothetical gene supported by AK123741	−4.7	0.0024	0.52	12q13.13
90	217428_s_at	NM_000493	COL10A1	Collagen, type X, alpha 1(Schmid metaphyseal chondrodysplasia)	−2.9	0.0025	0.52	6q22.1
94	222858_s_at	NM_014395	DAPP1	Dual adaptor of phosphotyrosine and 3-phosphoinositides	−3.7	0.0026	0.52	4q23
97	229849_at	—	—	Transcribed locus	−2.1	0.0028	0.52	7p15.1

[a]Genes are those in the top 100 t(12;14) UL-specific list (a more extensive list can be found as Supplementary Material).
[b]Dash indicates unknown.

Identification of t(12;14)-specific UL genes weighted for percent mosaicism of t(12;14) cells

Karyotypically abnormal UL are frequently found as mosaic tumors that include chromosomally normal cells. In contrast to previously published expression profiling studies, the impact of this biology was integrated by weighting each sample pair [t(12;14) UL and non-t(12;14) UL from the same uterus] for percent t(12;14) mosaicism of the tumor in a paired differential expression analysis: the higher the percentage of t(12;14) cells present, the more heavily weighted was that sample. The 50 most significant genes based on *Q*-value in this modified t(12;14) UL-specific gene list are given in Table 5. A more expansive list of 300 genes is also presented (Supplementary Material, Table S2). The top eight genes from this mosaicism-weighted list, which have significant *Q*-values of ≤0.10, are illustrated by scatter plots (Fig. 2A) with details tabulated (Fig. 2B). This demonstration of a relationship between expression and percent mosaicism suggests that weighting the samples for mosaicism level is necessary to compensate for background noise caused by the karyotypically normal cells in order to identify those genes specific to the t(12;14). The validity of this approach is supported by the movement of *HMGA2*, which is known to be highly up-regulated in t(12;14) UL, to the first position on the mosaicism-weighted list from its fifth position on the non-weighted list.

Quantitative polymerase chain reaction and immunohistochemistry confirmation of elevated *HMGA2* expression

In the nine cases investigated by microarray expression analysis, quantitative polymerase chain reaction (Q-PCR) confirmed that t(12;14) UL have significantly increased *HMGA2* mRNA compared with matched myometrium using a Wilcoxon signed-rank test (*P* = 0.0039). In addition, *HMGA2* mRNA in t(12;14) UL relative to matched myometrium was generally equivalent among tumors with >50% t(12;14) cells, suggesting a potential saturation effect in gene expression (Supplementary Material, Fig. S1). Elevated HMGA2 protein was also detected in t(12;14) UL relative to matched non-t(12;14) UL in both cases for which immunohistochemistry of paraffin sections was performed (an increase of 2.25-fold in Case 4 and of 1.77-fold in Case 5).

Q-PCR confirmation of elevated *CCND1* and *CCND2* RNA expression and immunohistochemistry confirmation of increased CCND1 protein expression

Cases 1, 4, 6, 8 and 9 for which additional RNA was available were evaluated by Q-PCR for expression of *CCND1* (cyclin D1). The 2.3-fold increase in RNA expression of *CCND1* in t(12;14) UL relative to matched non-t(12;14) tumors after normalization to the housekeeping gene *GAPDH* correlated with

Table 4. Genes up-regulated in t(12;14) UL compared with non-t(12;14) UL

Number[a]	Probe set	Ref. Seq.	Gene symbol	Gene title	Fold change	P-value	Q-value	Chromosome
1	220037_s_at	NM_006691	LYVE1	Lymphatic vessel endothelial hyaluronan receptor 1	3.2	3.70E − 06	0.082	11p15.4
3	214767_s_at	NM_144617	HSPB6	Heat shock protein, α-crystallin-related, B6	3.2	3.40E − 05	0.25	19q13.12
5	208025_s_at	NM_003483	HMGA2	High mobility group AT-hook 2	23	0.00017	0.43	12q14.3
6	211792_s_at	NM_001262	CDKN2C	Cyclin-dependent kinase inhibitor 2C (p18, inhibits CDK4)	4.4	2.00E − 04	0.43	1p33
7	240815_at	—[b]	—	Transcribed locus	2.5	0.00024	0.43	7q21.11
9	224438_at	—	—	—	3.4	0.00026	0.43	19q13.11
11	225954_s_at	NM_177401	MIDN	Midnolin	1.7	0.00035	0.43	19p13.3
12	221288_at	NM_005295	GPR22	G protein-coupled receptor 22	7.6	0.00036	0.43	7q22.3
14	237696_at	—	—	Transcribed locus	2.1	0.00036	0.43	4q12
15	231259_s_at	—	—	Transcribed locus	2	0.00036	0.43	12p13.32
16	243041_s_at	—	—	Transcribed locus	2.1	0.00037	0.43	3p24.1
17	212384_at	NM_004640	BAT1	HLA-B-associated transcript 1	2	0.00038	0.43	6p21.33
18	239999_at	NM_001005732	C21orf34	Chromosome 21 open reading frame 34	1.7	0.00039	0.43	21q21.1
19	208321_s_at	NM_001033677	CABP1	Calcium-binding protein 1	2.9	0.00039	0.43	12q24.31
21	225128_at	NM_153705	KDELC2	KDEL (Lys-Asp-Glu-Leu) containing 2	1.7	0.00043	0.44	11q22.3
22	204035_at	NM_003469	SCG2	Secretogranin II (chromogranin C)	4.7	0.00046	0.44	2q36.1
23	214989_x_at	—	—	CDNA FLJ11875 fis, clone HEMBA1007078	2.1	0.00047	0.44	12p12.3
24	205381_at	NM_001031692	LRRC17	Leucine-rich repeat containing 17	1.9	0.00049	0.44	7q22.1
25	1553179_at	NM_133638	ADAMTS19	ADAM metallopeptidase with thrombospondin type 1 motif, 19	2.5	0.00055	0.45	5q23.3
26	241509_at	—	—	—	2.7	0.00056	0.45	12p12.3
27	230577_at	—	—	Transcribed locus	6.7	0.00056	0.45	10q21.1
28	210202_s_at	NM_004305	BIN1	Bridging integrator 1	1.9	0.00066	0.5	2q14.3
29	1555250_a_at	NM_014912	CPEB3	Cytoplasmic polyadenylation element-binding protein 3	2.3	0.00067	0.5	10q23.32
30	238546_at	NM_001112800	SLC8A1	Solute carrier family 8 (sodium/calcium exchanger), member 1	1.9	0.00076	0.5	2p22.1
31	226304_at	NM_144617	HSPB6	Heat shock protein, α-crystallin-related, B6	2.5	0.00082	0.5	19q13.12
32	210230_at	—	—	CDNA: FLJ23438 fis, clone HRC13275	2.3	0.00084	0.5	17p13.3
33	207133_x_at	NM_001102406	ALPK1	α-Kinase 1	3.2	0.00084	0.5	4q25
35	243428_at	NR_002728	KCNQ1OT1	KCNQ1 overlapping transcript 1 (non-protein coding)	2.5	0.00091	0.5	11p15.5
37	226407_at	—	—	CDNA FLJ30519 fis, clone BRAWH2000859	2.4	0.00094	0.5	13q14.12
39	239910_at	NM_001031850	PSG6	Pregnancy specific β-1-glycoprotein 6	1.6	0.001	0.5	19q13.31
40	244614_at	NM_001007565	TFG	TRK-fused gene	2.2	0.0011	0.5	3q12.2
41	1554504_at	NM_005467	NAALAD2	N-acetylated α-linked acidic dipeptidase 2	2.5	0.0011	0.5	11q14.3
42	205677_s_at	NR_002605	DLEU1	Deleted in lymphocytic leukemia, 1	1.9	0.0011	0.5	13q14.3
43	200952_s_at	NM_001759	CCND2	Cyclin D2	3	0.0011	0.5	12p13.32
46	240245_at	—	—	—	2.2	0.0012	0.5	3p24.1
47	1556820_a_at	NR_002612	DLEU2	Deleted in lymphocytic leukemia, 2	1.7	0.0012	0.5	13q14.3
48	243874_at	NM_005578	LPP	LIM domain containing preferred translocation partner in lipoma	1.9	0.0012	0.5	3q28
49	237521_x_at	—	—	Transcribed locus	1.7	0.0012	0.5	11q23.3
50	227192_at	NM_145239	PRRT2	Proline-rich transmembrane protein 2	1.8	0.0012	0.5	16p11.2
52	241789_at	—	—	CDNA FLJ36544 fis, clone TRACH2006378	1.9	0.0013	0.5	3p24.1
53	208712_at	NM_053056	CCND1	cyclin D1	2.5	0.0013	0.5	11q13.2
54	202921_s_at	NM_001148	ANK2	Ankyrin 2, neuronal	2.4	0.0013	0.5	4q26
55	235133_at	—	—	*Homo sapiens*, clone IMAGE:5787583, mRNA	1.8	0.0013	0.5	6q25.3
56	229245_at	NM_014935	PLEKHA6	Pleckstrin homology domain containing, family A member 6	2	0.0013	0.5	1q32.1
58	1566163_at	—	—	Transcribed locus	1.9	0.0013	0.5	15q14
59	208711_s_at	NM_053056	CCND1	Cyclin D1	3.3	0.0014	0.5	11q13.2
60	213367_at	NR_015357	LOC791120	Hypothetical LOC791120	1.6	0.0014	0.5	7q36.1
62	223963_s_at	NM_001007225	IGF2BP2	Insulin-like growth factor 2 mRNA-binding protein 2	2.6	0.0014	0.5	3q27.2
63	232405_at	—	—	CDNA: FLJ22832 fis, clone KAIA4195	2.1	0.0014	0.5	4q26
65	242565_x_at	NM_001006114	C21orf57	Chromosome 21 open reading frame 57	1.6	0.0016	0.52	21q22.3

Continued

Table 4. *Continued*

Number[a]	Probe set	Ref. Seq.	Gene symbol	Gene title	Fold change	*P*-value	*Q*-value	Chromosome
66	1567224_at	NM_003483	HMGA2	High mobility group AT-hook 2	13	0.0017	0.52	12q14.3
67	227985_at	—	—	—	2.2	0.0017	0.52	7p15.3
68	219025_at	NM_020404	CD248	CD248 molecule, endosialin	1.6	0.0018	0.52	11q13.1
69	239320_at	NM_001080457	LRRC4B	Leucine-rich repeat containing 4B	2	0.0019	0.52	19q13.33
70	200953_s_at	NM_001759	CCND2	Cyclin D2	2.6	0.0019	0.52	12p13.32
71	1561657_at	—	—	Full-length insert cDNA clone YZ55H04	1.9	0.0019	0.52	11q23.1
72	242239_at	—	—	CDNA clone IMAGE:5314281	1.7	0.002	0.52	10p12.33
73	1562434_at	NM_001080419	UNK	Unkempt homolog (*Drosophila*)	2	0.002	0.52	17q25.1
74	220266_s_at	NM_004235	KLF4	Kruppel-like factor 4 (gut)	1.6	0.002	0.52	9q31.2
75	239281_at	—	—	*Homo sapiens*, clone IMAGE:5787583, mRNA	1.8	0.002	0.52	6q25.3
76	201282_at	NM_001003941	OGDH	Oxoglutarate (α-ketoglutarate) dehydrogenase (lipoamide)	2.1	0.002	0.52	7p13
78	224566_at	NR_002802	TncRNA	Trophoblast-derived non-coding RNA	2.1	0.0021	0.52	11q13.1
79	227835_at	XM_001722051	LOC100132181	Hypothetical protein LOC100132181	1.7	0.0021	0.52	17p13.3// 7p22.3
80	202672_s_at	NM_001030287	ATF3	Activating transcription factor 3	2.1	0.0022	0.52	1q32.3
81	238447_at	NM_001003792	RBMS3	RNA-binding motif, single-stranded interacting protein	1.8	0.0022	0.52	3p24.1
82	219370_at	NM_019845	RPRM	Reprimo, TP53-dependent G2 arrest mediator candidate	1.7	0.0023	0.52	2q23.3
83	203186_s_at	NM_002961	S100A4	S100 calcium-binding protein A4	3.2	0.0023	0.52	1q21.3
84	219089_s_at	NM_024327	ZNF576	Zinc finger protein 576	1.5	0.0023	0.52	19q13.31
85	241345_at	NM_005455	ZRANB2	Zinc finger, RAN-binding domain containing 2	2.1	0.0023	0.52	1p31.1
86	215303_at	NM_004734	DCLK1	Doublecortin-like kinase 1	1.6	0.0023	0.52	13q13.3
87	1559891_at	NM_003483	HMGA2	High-mobility group AT-hook 2	3.4	0.0024	0.52	12q14.3
89	200951_s_at	NM_001759	CCND2	cyclin D2	2.7	0.0025	0.52	12p13.32
91	240452_at	NM_002094	GSPT1	G1 to S phase transition 1	1.7	0.0025	0.52	16p13.13
92	219059_s_at	NM_006691	LYVE1	Lymphatic vessel endothelial hyaluronan receptor 1	2.1	0.0026	0.52	11p15.4
93	241817_at	NM_198562	C3orf62	Chromosome 3 open reading frame 62	1.7	0.0026	0.52	3p21.31
95	206738_at	NM_001646	APOC4	Apolipoprotein C-IV	1.6	0.0027	0.52	19q13.32
96	241752_at	NM_001112800	SLC8A1	Solute carrier family 8 (sodium/calcium exchanger), member 1	2	0.0027	0.52	2p22.1
98	228632_at	—	—	CDNA FLJ37243 fis, clone BRAMY2004387	2.4	0.0028	0.52	14q32.31
99	225660_at	NM_020796	SEMA6A	Sema domain, transmembrane domain (TM), and cytoplasmic domain, (semaphorin) 6A	1.9	0.0028	0.52	5q23.1
100	214657_s_at	NR_002802	TncRNA	Trophoblast-derived non-coding RNA	2.3	0.0028	0.52	11q13.1

[a]Genes are those in the top 100 t(12;14) UL-specific list (a more extensive list can be found as Supplementary Material).
[b]Dash indicates unknown.

the 2.9-fold elevation in expression detected by microarray after averaging the fold change of all probe sets in *CCND1*. Similarly examined was *CCND2* (cyclin D2), which showed a 1.8-fold expression increase by Q-PCR in t(12;14) UL, consistent with the finding by microarray of a 2.1-fold higher average expression across all probe sets. Evaluation of CCND1 protein by immunohistochemistry with manual scoring confirmed increased expression in t(12;14) UL relative to matched non-t(12;14) UL (an elevation of 12.50-fold in Case 4 and of 3.84-fold in Case 5); both cases were previously shown in a semi-automated analysis to have a similar HMGA2 protein distribution pattern.

Functional significance of t(12;14)-specific UL genes

To extract biological insight from the transcriptional profile of t(12;14) UL, the 374 probe sets with $P \leq 0.005$ from the t(12;14) mosaicism-weighted gene list were investigated with Ingenuity Pathways Analysis (IPA). IPA is a web-supported tool based on a database of functional relationships between genes manually curated from scientific publications. There were 13 highly significant networks of dependencies generated, each involving 7–25 genes from the t(12;14) UL-specific list. The two most significant networks (Fig. 3A and B) are principally associated with cell proliferation and development. The other networks involving 7–20 t(12;14) UL-specific genes are generally associated with cell cycle, growth and signaling, cancer, cell and tissue morphology, nucleic acid and lipid metabolism, developmental and other disorders, and normal development pathways of multiple different systems. Among well-characterized canonical pathways, cell cycle G1/S checkpoint regulation was the most significant ($P = 0.0042$), involving increased expression of

Table 5. Genes up- or down-regulated in t(12;14) UL compared with non-t(12;14) UL weighted for percent mosaicism

Number[a]	Non-weighted[b]	Probe set	Ref. Seq.	Gene symbol	Gene title	Fold change[c]	P-value	Q-value	Chromosome
1	5	208025_s_at	NM_003483	HMGA2	High mobility group AT-hook 2	49	2.90E − 06	0.035	12q14.3
2	9	224438_at	—[d]	—	—	4	4.10E − 06	0.035	19q13.11
3	20	211276_at	NM_080390	TCEAL2	Transcription elongation factor A (SII)-like 2	−7.6	5.70E − 06	0.035	Xq22.1
4	10	222549_at	NM_021101	CLDN1	Claudin 1	−7.5	6.20E − 06	0.035	3q28
5	4	238018_at	NM_001002919	FAM150B	Family with sequence similarity 150, member B	−5.5	1.10E − 05	0.05	2p25.3
6	1	220037_s_at	NM_006691	LYVE1	Lymphatic vessel endothelial hyaluronan receptor 1	3.1	1.50E − 05	0.056	11p15.4
7	12	221288_at	NM_005295	GPR22	G protein-coupled receptor 22	10	2.30E − 05	0.073	7q22.3
8	59	208711_s_at	NM_053056	CCND1	Cyclin D1	4	3.40E − 05	0.095	11q13.2
9	81	238447_at	NM_001003792	RBMS3	RNA-binding motif, single-stranded interacting protein	2.1	4.60E − 05	0.11	3p24.1
10	2	225619_at	NM_001040153	SLAIN1	SLAIN motif family, member 1	−3.1	5.30E − 05	0.12	13q22.3
11	87	1559891_at	NM_003483	HMGA2	High mobility group AT-hook 2	4.8	5.90E − 05	0.12	12q14.3
12	53	208712_at	NM_053056	CCND1	Cyclin D1	3.2	7.30E − 05	0.12	11q13.2
13	45	230353_at	—	LOC284112	Hypothetical protein LOC284112	−3	7.70E − 05	0.12	17p13.2
14	89	200951_s_at	NM_001759	CCND2	cyclin D2	3.3	7.80E − 05	0.12	12p13.32
15	3	214767_s_at	NM_144617	HSPB6	Heat shock protein, α-crystallin-related, B6	3.1	7.80E − 05	0.12	19q13.12
16	150	204359_at	NM_013231	FLRT2	Fibronectin leucine-rich transmembrane protein 2	−2.9	1.00E − 04	0.12	14q31.3
17	43	204359_at	NM_001759	CCND2	Cyclin D2	3.2	0.00011	0.12	12p13.32
18	32	210230_at	—		CDNA: FLJ23438 fis, clone HRC13275	2.8	0.00011	0.12	17p13.3
19	6	211792_s_at	NM_001262	CDKN2C	Cyclin-dependent kinase inhibitor 2C (p18, inhibits CDK4)	5	0.00011	0.12	1p33
20	521	218182_s_at	NM_021101	CLDN1	Claudin 1	−6.4	0.00011	0.12	3q28
21	8	219290_x_at	NM_014395	DAPP1	Dual adaptor of phosphotyrosine and 3-phosphoinositides	−4	0.00012	0.12	4q23
22	58	1566163_at	—	—	Transcribed locus	2	0.00013	0.13	15q14
23	52	241789_at	—		CDNA FLJ36544 fis, clone TRACH2006378	1.9	0.00017	0.17	3p24.1
24	456	222940_at	NM_005420	SULT1E1	Sulfotransferase family 1E, estrogen-preferring, member 1	−4.2	0.00019	0.17	4q13.3
25	18	239999_at	NM_001005732	C21orf34	Chromosome 21 open reading frame 34	1.7	2.00E − 04	0.17	21q21.1
26	15	231259_s_at	—	—	Transcribed locus	2	2.00E − 04	0.17	12p13.32
27	64	219737_s_at	NM_020403	PCDH9	Protocadherin 9	−3.3	0.00022	0.18	13q21.32
28	57	226231_at	—	—	Transcribed locus	−3.3	0.00027	0.19	20q13.12//12q21.2
29	46	240245_at	—	—	—	2.3	0.00032	0.19	3p24.1
30	71	1561657_at	—	—	Full-length insert cDNA clone YZ55H04	2.2	0.00034	0.19	11q23.1
31	394	243808_at	—	—	Transcribed locus	2.4	0.00035	0.19	7q21.2
32	14	237696_at	—	—	Transcribed locus	2	0.00035	0.19	4q12
33	7	240815_at	—	—	Transcribed locus	2.5	0.00035	0.19	7q21.11
34	22	204035_at	NM_003469	SCG2	Secretogranin II (chromogranin C)	4.8	0.00035	0.19	2q36.1
35	16	243041_s_at	—	—	Transcribed locus	2.2	0.00036	0.19	3p24.1
36	34	229515_at	NM_002583	PAWR	PRKC, apoptosis, WT1, regulator	−1.9	0.00037	0.19	12q21.2
37	67	227985_at	—	—	Transcribed locus	2.3	0.00037	0.19	7p15.3
38	70	200953_s_at	NM_001759	CCND2	cyclin D2	3.2	0.00037	0.19	12p13.32
39	21	225128_at	NM_153705	KDELC2	KDEL (Lys-Asp-Glu-Leu) containing 2	1.6	0.00038	0.19	11q22.3
40	61	226863_at	NM_001077710	FAM110C	Family with sequence similarity 110, member C	−2.5	0.00038	0.19	2p25.3
41	949	205347_s_at	NM_021992	TMSL8	Thymosin-like 8 /// thymosin β15b	−2.2	0.00038	0.19	Xq22.1
42	228	1556069_s_at	NM_022462	HIF3A	Hypoxia-inducible factor 3, α-subunit	2.4	0.00039	0.19	19q13.32
43	200	218847_at	NM_001007225	IGF2BP2	Insulin-like growth factor 2 mRNA-binding protein 2	6.2	0.00039	0.19	3q27.2
44	77	228155_at	NM_032333	C10orf58	Chromosome 10 open reading frame 58	−1.9	4.00E − 04	0.19	10q23.1
45	31	226304_at	NM_144617	HSPB6	Heat shock protein, α-crystallin-related, B6	2.6	4.00E − 04	0.19	19q13.12
46	48	243874_at	NM_005578	LPP	LIM domain containing preferred translocation partner in lipoma	2	0.00041	0.19	3q28
47	252	240813_at	—	—	Transcribed locus	2.1	0.00041	0.19	11q23.1
48	24	205381_at	NM_001031692	LRRC17	Leucine-rich repeat containing 17	2	0.00041	0.19	7q22.1
49	11	225954_s_at	NM_177401	MIDN	Midnolin	1.7	0.00042	0.19	19p13.3
50	517	33767_at	NM_021076	NEFH	neurofilament, heavy polypeptide 200 kDa	−2.5	0.00043	0.19	22q12.2

[a]Genes are those in the top 50 t(12;14) UL-specific list that have been weighted for the percent mosaicism (a more extensive list can be found as Supplementary Material).
[b]Number on non-weighted t(12;14) UL-specific gene list.
[c]Expression fold change between t(12;14) and non-t(12;14) UL weighted for percent mosaicism.
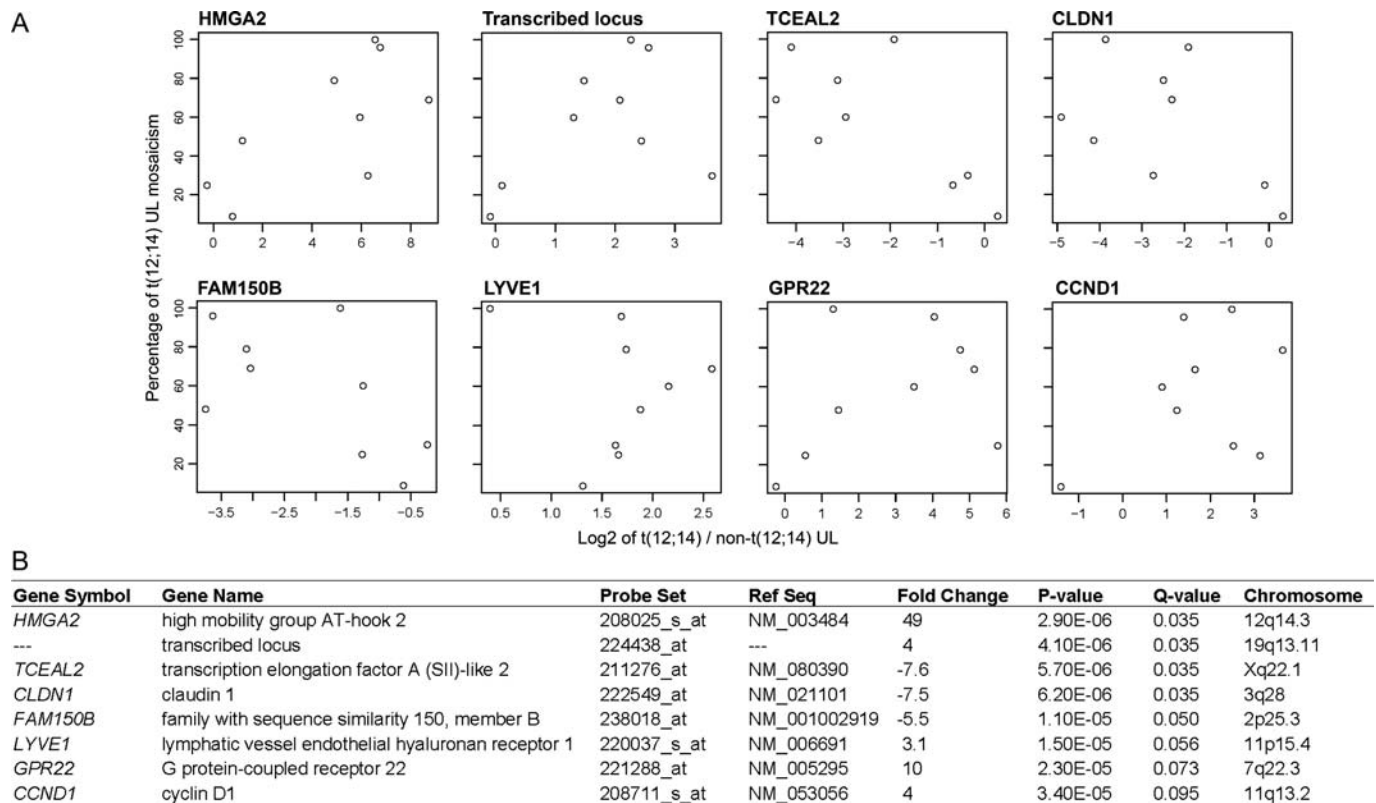[d]Dash indicates unknown.

Figure 2. Weighting the microarray data for the level of t(12;14) cell mosaicism in each UL results in identification of eight significant genes with a *Q*-value of ≤0.10. (**A**) Scatter plots show the relationship between the percent of t(12;14) cells and the log$_2$ fold change ratio of gene expression in t(12;14) UL relative to the non-t(12;14) UL in each of the nine women. (**B**) Details about the eight genes, which include *HMGA2* and *CCND1*.

four t(12;14) UL-specific genes: *CCND1*, *CCND2*, *CCND3* and *CDK6*.

Gene Set Enrichment Analysis (GSEA) was also employed which uses a continuum of differential expression scores for all genes rather than dividing the genes into significant versus non-significant categories (34). Application of GSEA to the mosaicism-weighted t(12;14) UL-specific gene list identified significant enrichment (a false discovery rate of <0.2) for eight gene sets including two associated with mitotic cell cycle (G1/S checkpoint and interphase), which is consistent with the IPA (Fig. 4). The six other significant gene sets were primarily associated with GTPase or kinase activity, possibly indicating additional molecular pathways differentially activated between t(12;14) and non-t(12;14) UL.

Menopause or medications creating a hypogonadal state do not appear to significantly alter the t(12;14) expression analysis

UL are hormonally responsive to the gonadal steroids estrogen and progesterone, and four of the nine women in this study were menopausal or on medications creating a hypogonadal state at the time of tumor collection (Table 2). Thus, an assessment was undertaken of whether the same genes are significantly changed when only the non-menopausal/non-medicated subset is examined. The mosaicism-weighted fold changes (log$_2$ scale) between the whole data set ($n = 9$) and the non-menopausal/non-medicated subset ($n = 5$)

showed a high Pearson's correlation ($r = 0.875$). Further, both in total and non-menopausal/non-medicated cases, the top variable probes corresponded to *HMGA2* (Supplementary Material, Fig. S2). As anticipated, the results favor the premise that a paired comparison of a t(12;14) UL and a non-t(12;14) UL from each woman neutralizes environmental influences such as menopausal status from significantly affecting the gene expression analysis. In addition, application of GSEA to only the non-menopause data subset confirmed the importance of the mitotic G1/S checkpoint with a false discovery rate of 0.18.

Genetic heterogeneity among UL subgroups

After combining the t(12;14) UL expression data set with the previously published del(7q) UL data set (GEO accession GSE12814) (32), the top 1000 most variable genes were selected for an unsupervised hierarchical cluster analysis with adjustment for batch effect (Fig. 5) (35). The results substantiate the previous findings of the individual t(12;14) or del(7q) analyses where myometrium samples largely separated from the tumors while the tumors generally clustered by patient rather than by non-t(12;14)/non-del(7q) versus t(12;14)/del(7q) status. In addition, although there was not a distinct separation of t(12;14) and del(7q) tumors, the weighted t(12;14) UL- and the weighted del(7q) UL-specific gene lists were mutually exclusive (i.e., only three common genes were observed between the top 500 genes; *P*-value of
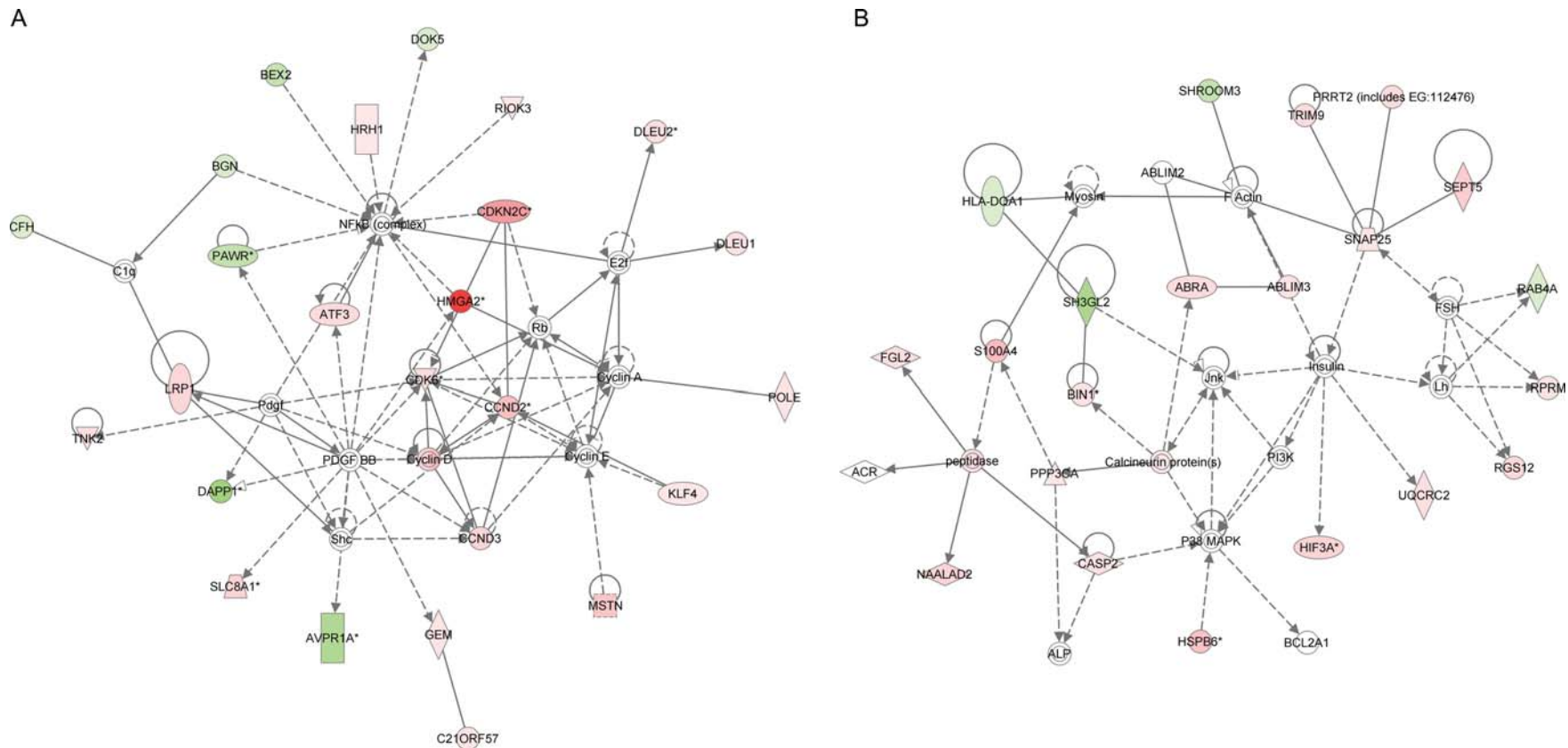
Figure 3. The use of IPA to identify highly significant networks of functional dependencies of genes represented by the 374 probe sets with a *P*-value of ≤0.005 from the t(12;14) UL-specific gene list weighted for percent of t(12;14) cells. The functions of the two networks of highest significance are involved in (**A**) cell development, cell proliferation and respiratory system development and function [score = 46, genes from t(12;14) list = 25], which includes *HMGA2*, and (**B**) cellular assembly and organization, and embryonic and organ development [score = 36, genes from t(12;14) list = 21]. Each node in the network corresponds to a gene and each arc to a published article reporting a functional relationship between those two linked genes. Pink shading indicates up-regulated gene expression, green shading down-regulated gene expression, solid lines a direct relationship between connected genes and dotted lines an indirect relationship between linked genes.
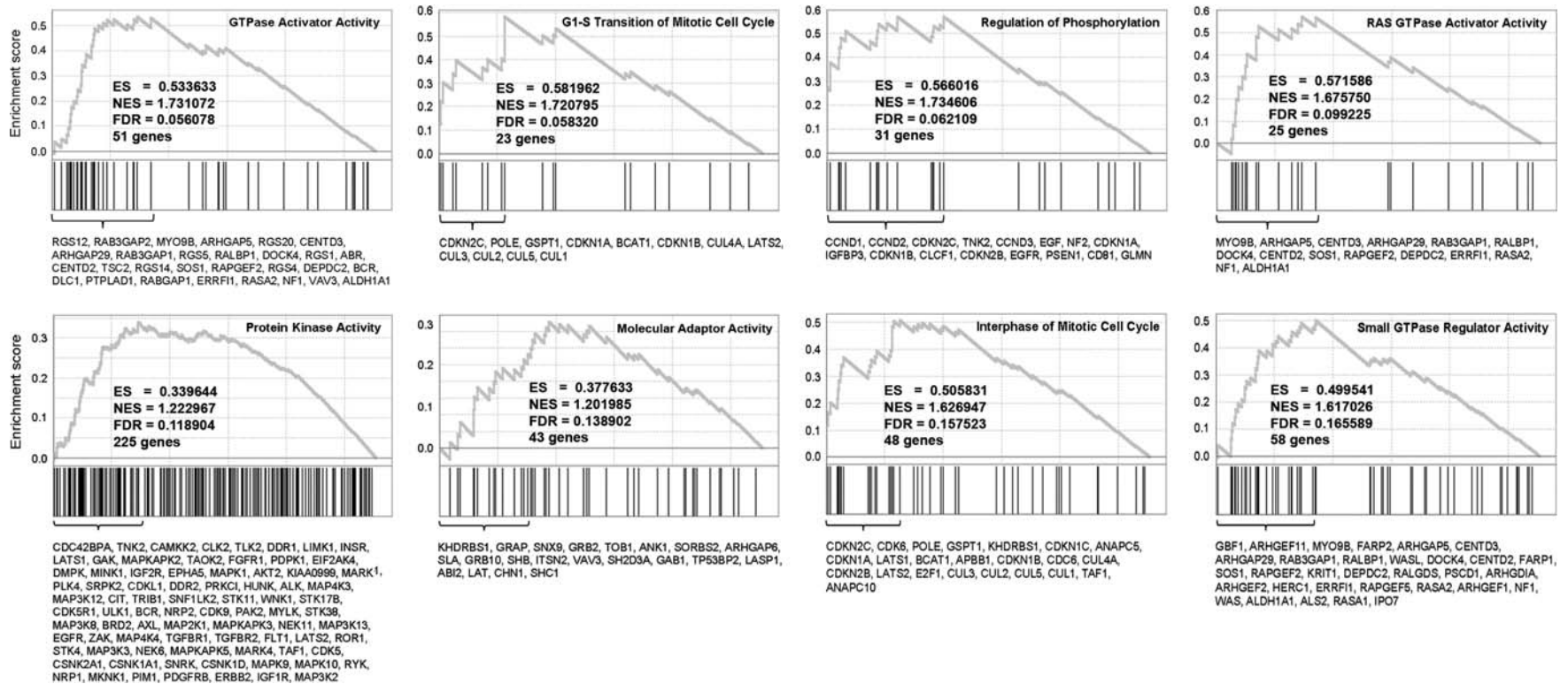
Figure 4. GSEA found eight molecular functions, including two involving the cell cycle, significantly enriched with genes which were differentially expressed between t(12;14) UL and non-t(12;14) UL based on a false discovery rate (FDR) of <0.2. Plots of these eight molecular functions show the enrichment score (*y*-axis) across the genes (*x*-axis) sorted in the order of differential expression (upper section, each panel). Vertical bars represent genes that belong to the functional set (middle section, each panel). The leading edge gene subset is provided as a list of gene symbols (bottom section, each panel). The peak value of the enrichment score is reported as ES and the normalized value as NES.
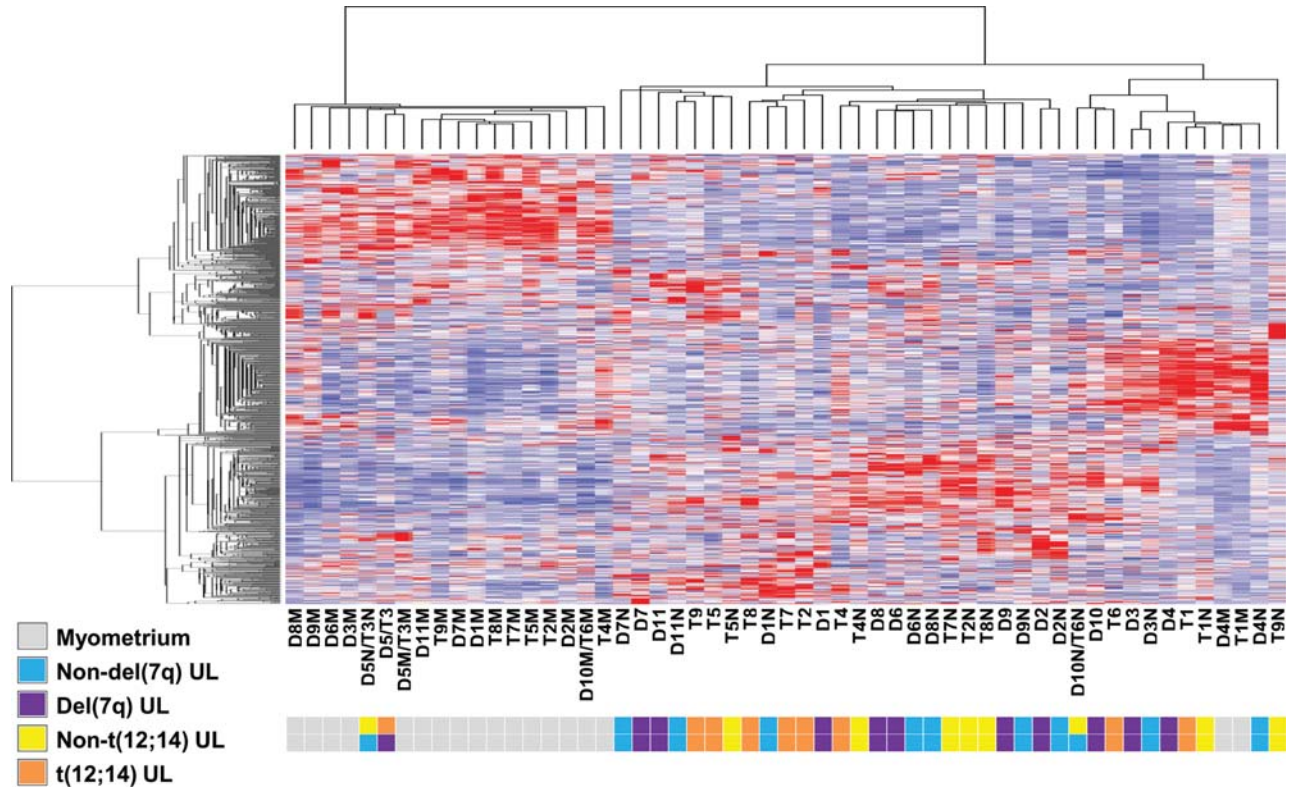
Figure 5. Merging the microarray expression profiles of the t(12;14) and del(7q) data sets confirmed the need for paired analysis to control for patient-to-patient variability and demonstrated a potential underlying genetic predisposition to these karyotypic abnormalities based on the clustering pattern of their myometrial samples. A heatmap of an unsupervised hierarchical cluster analysis of the 1000 most variable genes between t(12;14) UL [T (translocation) followed by the case number], non-t(12;14) UL [N (non) following T and the case number] and myometrium [M following T and the case number] from each of the 9 women in the t(12;14) data set as well as del(7q) UL [D (deletion) followed by the case number], non-del(7q) UL [N following D and the case number] and myometrium [M following D and the case number] from each of 11 women in the del(7q) data set. Of note, one case is a mosaic t(12;14)/del(7q) UL which is denoted as D5/T3, D5N/T3N and D5M/T3M and is included in the combined analysis only once. Also, one case had a t(12;14) UL [designated T6] and a separate del(7q) UL [designated D10] within the same uterus, and therefore these tumors have in common a myometrium [designated D10M/T6M] and a non-t(12;14)/ non-del(7q) sample [designated D10N/T6N] which are included in the combined analysis only once. As was previously observed in the individual analyses, a trend of myometrial separation from all UL tissues and of UL clustering based on patient rather than t(12;14) or del(7q) status was found. In addition, the myometrium samples generally clustered based on their associated tumor karyotypic abnormality.

exclusivity = 0.0071 using Fisher's exact test). These results indicate patient bias (constitutional genetics and/or environmental exposures) likely significantly interferes with identifying the transcriptional effects of the t(12;14) and del(7q) somatic changes, suggesting the necessity of matched sample analysis to remove this bias.

Genetic heterogeneity among myometrial samples

The myometrium samples not only segregated from the tumors, but within the myometrium group, t(12;14) patients generally clustered separately from the del(7q) patients even after batch effect correction (Fig. 5). The ability to distinguish myometrium obtained from t(12;14) UL patients versus those with del(7q) UL was confirmed by the finding of 100% accuracy to call the tumor karyotypic abnormalities associated with each myometrium sample using a leave-one-out cross-validation test [$n = 7$ t(12;14) patients and $n = 9$ del(7q) patients]. Myometrium samples excluded from this analysis were from two patients with both a t(12;14) and a del(7q) tumor (samples D5M/T3M and D10M/T6M). Nine genes were identified using the *k*-NN (*k*-nearest neighbor) method

that can distinguish the myometrium origin and are illustrated with a heatmap (Fig. 6).

DISCUSSION

Identification of recurrent primary chromosome abnormalities in UL suggests that these tumors arise through multiple genetic pathways. One major UL cytogenetic subgroup, t(12;14)(q14-15;q23-24), has the pathogenetic target *HMGA2* that is involved in multiple mesenchymal solid tumors (36,37). The presence of t(12;14) in UL leads to elevated expression of *HMGA2* (14,15). Real-time PCR and immunohistochemistry in the current investigation confirmed increased *HMGA2* in t(12;14) UL relative to matched non-t(12;14) UL and myometrium. Elevated *HMGA2* has also been noted in many malignant tumors (38).

In the present study, a molecular signature of t(12;14) UL was identified by directly comparing expression profiles of t(12;14) UL and non-t(12;14) UL removed concurrently from the same uterus in each of nine women. This approach is different from previously published expression studies
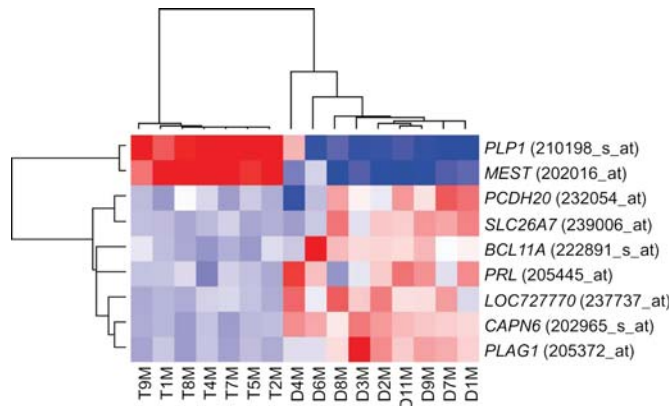
Figure 6. Nine genes distinguish the myometrial origin from t(12;14) UL or del(7q) UL patients. A heatmap showing the expression signature of these nine genes in the myometrium from each of seven women with t(12;14) UL and nine women with del(7q) UL. The myometrium from two patients were excluded due to the presence of both a t(12;14) and a del(7q) tumor (samples D5M/T3M and D10M/T6M).

which compare UL with normal myometrial tissue. Our data demonstrated that t(12;14) UL and non-t(12;14) UL clustered separately from myometrium, which suggests that expression profiling of myometrium does not help elucidate t(12;14) UL-specific genes. UL were also noted to generally cluster by patient rather than t(12;14) versus non-t(12;14) status, suggesting a need to control for patient variability caused by genetic and environmental factors such as menstrual cycle status. Therefore, a paired comparison of t(12;14) UL to non-t(12;14) UL to increase specificity was used to develop a molecular signature of the t(12;14) abnormality. In addition, data were further refined through weighting based on the percent of abnormal t(12;14) cells in each neoplasm to account for the mosaic nature of UL.

The need for a paired design is illustrated by the finding that menopause, the absence of steroid hormones which are a known environmental influence on UL growth, does not appear to significantly affect the t(12;14) gene list in this study. This was demonstrated by a significant correlation in gene expression between the non-menopausal case subset and the whole data set, including *HMGA2* as the most highly expressed transcript in both groups.

To study further the genetic expression of t(12;14) UL, this data set including the myometrium was combined with that of a previously published 7q22 deletion cytogenetic subgroup (32), and an unsupervised hierarchical cluster analysis was performed. The tumors tended to cluster by patient rather than by the presence or absence of the cytogenetic abnormality. The t(12;14) UL were also not clearly distinguishable from the del(7q) UL. This suggests that patient variability due to constitutional genetics and/or environment has a predominant effect, and therefore, a paired analysis is likely required to determine t(12;14) UL-specific genes. This patient variability effect is so strong that in a single case with independent del(7q) and t(12;14) UL [Case 6 in Table 1 and Case 10 in (32)], it was found that those tumors clustered together along with the non-del(7q)/non-t(12;14) UL from the same woman (D10, T6, D10N/T6N in Fig. 5). In addition, the

single tumor that is a low-level mosaic for both del(7q) and t(12;14) [Case 3 in Table 1 and Case 5 in (32)] presented within the myometrium branch (D5/T3, D5N/T3N, D5M/T3M in Fig. 5), suggesting the genetic effects of both cytogenetic abnormalities are diluted by the mosaicism with each other and with normal cells.

A second result of this analysis was the finding that within the myometrium cluster, t(12;14) patients generally gathered separately from the del(7q) patients. Nine genes were identified that could predict whether a myometrium sample came from a woman with a t(12;14) UL versus a woman with a del(7q) UL. This suggests that there are different constitutional genetic predisposition alleles in women for these specific cytogenetic subgroups. Alternative potential mechanisms affecting myometrium expression can include a paracrine effect of UL with different cytogenetic abnormalities on adjacent myometrium or unappreciated microscopic UL in one or more of the myometrial samples. Precedent for general UL genetic predisposition was established by a genome-wide association study in which three loci were significantly associated with UL susceptibility (39). Further investigations are required to determine whether genetic predilection to UL formation in general is related to the potential constitutional predisposition to specific cytogenetic abnormalities in UL.

Among the nine genes that can differentiate between the myometrium of t(12;14) and del(7q) patients, *PLAG1* (pleomorphic adenoma gene 1) is significant as this proto-oncogene is ectopically overexpressed through recurrent translocations or amplifications in multiple neoplasms. Pleomorphic adenoma of the salivary gland is one such tumor; this benign growth is of particular interest as a subset harbor *HMGA2* rearrangement similar to the t(12;14) subgroup of UL (40). Further, like *HMGA2*, the expression of *PLAG1* is usually restricted to fetal development (41). *PLAG1* has also been shown to drive cell proliferation and oncogenic transformation, likely through its known mitogenic target genes such as *IGF2* (42,43). In fact, *PLAG1* increases proliferation by inducing G1/S transition in hematopoietic progenitors in cooperation with *CBFB*/*MYH11* fusion (44) and its disruption in mice results in growth retardation (41). These roles are interesting to consider in relation to *PLAG1* expression in the myometrium, and the question remains whether there is any relationship between *PLAG1* and *HMGA2* in pleomorphic adenomas or other tumors such as UL.

Another gene of interest in the myometrial differential data set, *PRL* (prolactin), induces phosphorylation of mitogen-activated protein (MAP) kinase and DNA synthesis in UL-derived smooth muscle cells (45). This suggests that *PRL* promotes UL cell proliferation via the MAP kinase cascade. Myometrial and UL cells were further shown to express the PRL receptor and to have a significant decrease in cell number *in vitro* after treatment with anti-PRL antibody (46). Therefore, even a modest overproduction of the stimulatory growth factor PRL in the myometrium could result through an autocrine mechanism in sustained, self-stimulated proliferation, predisposing to tumor formation.

Other genes among the nine that are of potential relevance include *MEST*, *CAPN6* and *BCL11A* due to their known neoplastic associations. *MEST* (mesoderm-specific transcript) is overexpressed in UL relative to myometrium across multiple

expression array studies (47) and is also involved in proliferation as mice lacking *MEST* demonstrate growth retardation (48). *CAPN6* (calpain 6) is also overexpressed in UL relative to myometrium (49) and supports tumorigenesis through apoptosis inhibition and angiogenesis promotion (50). *BCL11A* (B-cell lymphoma/leukemia 11A) codes for a proto-oncogene transcription factor which is rearranged or amplified in a variety of B-cell malignancies (51).

The myometrium of the del(7q) and t(12;14) UL cytogenetic subgroups not only differ, but in contrast to the expression profile of del(7q) (32), the mosaicism-weighted t(12;14) UL-specific gene list suggests that cell cycle regulation is of primary importance. Application of IPA to the significant probe sets ($P \leq 0.005$) indicates that the top networks are principally associated with cell proliferation and development while the most-related canonical pathway is G1/S checkpoint regulation. Consistently, application of another functional analysis method, GSEA, showed significant enrichment for mitotic cell cycle function, particularly G1/S transition and interphase. Interestingly, when GSEA analysis was applied to only the subset of women who were non-menopausal, the significance of the mitotic G1/S transition function remained.

During the G1 phase of the cell cycle, D-type cyclins accumulate in response to growth signals and activate their associated cyclin-dependent kinases (CDKs), promoting progression through the restriction point to achieve S phase commitment and mitogen independence. In t(12;14) UL, the genes significantly up-regulated include multiple D-type cyclins (*CCND1*, *CCND2*, *CCND3*) and a CDK (*CDK6*). Overexpression of *CDK6* or *CCND1* has been shown to shorten the G1 phase and accelerate the G1/S transition (52,53). In addition, increased *CDK6* expression was observed in squamous cell carcinomas, gliomas and neuroblastomas while *CCND1* expression is characteristically elevated in multiple primary human tumors and cell lines (54−57).

Additional support for a relationship between t(12;14) and the cell cycle is shown by the marked growth advantage of t(12;14) UL, which was found in a systematic study of all palpable UL from hysterectomy specimens to be significantly larger in size than those with either interstitial 7q22 deletions or normal karyotypes (11). This may be directly related to increased expression of *HMGA2*, which has been identified as a delayed early response gene in multiple cell types (58−61). Since delayed early response genes normally promote progression to S phase in response to growth factors, UL cells with up-regulation of *HMGA2* due to t(12;14) may bypass the need for mitogen stimulation.

This connection between *HMGA2* and the cell cycle is also shown by insertional mutagenesis of *HMGA2* in mice which have significantly reduced body size as a result of widespread mesenchymal tissues growth restriction (21). A gene directly regulated by *HMGA2* and known to have decreased expression in these *pygmy* mice is insulin-like growth factor II mRNA-binding protein 2 (62,63). In the current study, *IMP2* (also known as *IGF2BP2*) is number 43 on the mosaicism-weighted t(12;14) UL-specific gene list with a significant 6.2-fold increase in expression relative to non-t(12;14) UL ($P = 0.00039$). *IMP2* encodes a mRNA-binding protein involved in regulating post-transcriptional processes, including influencing the major fetal period growth factor IGF-II (64). *IMP2*

may therefore function as an effector through which *HMGA2* contributes to growth in t(12;14) UL.

HMGA2 or other t(12;14)-associated genes may also potentially contribute to an injury-like response in UL as is known to occur during normal menstruation when increased uterine vasoconstrictive substances induce myometrial cell hypoxia (65). Decreased oxygen levels activate hypoxia-inducible factors (HIFs) which in turn induce transcription of genes involved in many functions including angiogenesis and cell survival (66). *HIF1A* is key in the initial adaptation of cells to an oxygen-poor environment, but recent data suggest that *HIF3A* takes over in maintaining long-term response to hypoxia (67). In the current study, *HIF3A* is a significant t(12;14) UL-specific gene, at number 24 with 2.4-fold increased expression ($P = 0.00039$) as well as being present four additional times in the top 437 probes with an overall average fold-change of 2.1 on the mosaicism-weighted gene list. IPA indicated *HIF3A* as a gene involved in the second most significant network. *HIF3A* may not only have a tumorigenic function but, as larger tumors are prone to hypoxia at their core and t(12;14) UL are known to generally be larger, t(12;14)-induced expression of *HIF3A* may allow UL with this translocation to remain viable during hypoxia-inducing rapid growth.

In conclusion, this study provides an expression profile of the t(12;14) cytogenetic subgroup of UL. The unique design employed to target t(12;14) UL-specific genes included a paired comparison to non-t(12;14) UL from the same women and weighting of the data for percent of t(12;14) cells to account for mosaicism with normal cells. This paired strategy was demonstrated to be required to remove the significant impact of patient variability. The resultant gene list with the known t(12;14)-associated gene *HMGA2* as the most significant gene strongly implicates the importance in t(12;14) UL of the G1−S cell cycle checkpoint. By examining expression profiles of morphologic variants and recurrent cytogenetic subgroups of UL, it is becoming clear that UL is not a single disease. In fact, analysis of myometrium from t(12;14) and del(7q) UL cases suggests distinct constitutional genetic predisposition for these somatic changes. Recognizing this genetic heterogeneity and establishing genetic profiles of the different entities are taking the first steps toward understanding the implications of how genetic variability impacts disease occurrence, severity and recurrence, particularly as less invasive uterus-sparing procedures are becoming the standard of care.

MATERIALS AND METHODS

Clinical material

For each woman, the total number of tumors present were counted and tissue was obtained from the myometrium and a minimum of three UL (as in Cases 1−3) or up to five UL when available (as in Cases 4−9), selecting the tumor with the largest diameter first and others in a descending size order. All collected tumors were then screened for t(12;14)(q14-15;q23-24) and del(7)(q22q32) using GTG-banded karyotyping according to established protocols (9) or FISH. Selection of cases for further studies required

the t(12;14) UL had matched myometrium and non-t(12;14) UL samples acquired and screened concurrently with the karyotypically abnormal tumor. Two UL with t(12;14) (Cases 1 and 2) and one UL that was mosaic for both t(12;14) and del(7q) (Case 3) were obtained from surgical specimens at Brigham and Women's Hospital (BWH) through a Partners HealthCare IRB-approved protocol between 1990 and 2004. Six UL with t(12;14) (Cases 4–9) were identified from an IRB-approved tissue bank of over 100 consented, premenopausal, 25- to 50-year-old women who underwent myomectomy or hysterectomy at BWH between 2003 and 2007. Diagnosis of UL was confirmed through medical record review. Participants consented for the tissue bank also completed detailed epidemiological questionnaires surveying clinical, reproductive, sexual, dietary and family history. Each case was grossly confirmed to be a UL or myometrial specimen, and when possible, hematoxylin- and eosin-stained tissue sections underwent pathologic evaluation (Table 1).

Fluorescence *in situ* hybridization

End-sequenced and FISH-verified bacterial artificial chromosomes (68) were selected using the University of California Santa Cruz Biotechnology Genome Browser and Database (http://genome.ucsc.edu) (69) and then obtained from the RP11 library (BACPAC Resource Center at the Children's Hospital Oakland Research Institute, Oakland, CA, USA) or the CTD library (Invitrogen). DNA was isolated from bacterial cultures following a standard protocol consisting of alkaline lysis, neutralization and ethanol precipitation.

UL with t(12;14)(q14-15;q23-24) were identified by the presence of a fusion signal of probes RP11-185D13 located at 12q14.3 and CTD-3225F7 at 14q24 by interphase FISH on nuclei from fresh fixed cell pellets as described previously (70). A total of 100 interphase nuclei were scored for each specimen. The probe set was validated on both normal metaphases from peripheral blood lymphocytes and on interphase nuclei from karyotype-confirmed t(12;14) UL.

Immunohistochemistry for HMGA2

Detection of HMGA2 protein in formalin-fixed, paraffin-embedded t(12;14) UL and matched non-t(12;14) UL tissue sections for Cases 4 and 5 involved pressure cooker heat-induced antigen retrieval for 2 min in citrate buffer followed by a 20 min cool down, a 5 min 0.05 M Tris/Tween 20 wash, a 5 min peroxidase block (Dako) and a 5 min Tris incubation. A 1:2000 dilution of a primary polyclonal anti-HMGA2 antibody (Biocheck, Inc.) was used for 40 min. The Envision Plus detection system (Dako) was then applied, including a 30 min incubation with goat anti-rabbit immunoglobulin conjugated to a peroxidase-labeled polymer [horseradish peroxidase (HRP)] followed by a 5 min exposure to the substrate diaminobenzidine (DAB) to produce a brown precipitate visible by microscopy. Hematoxylin was used as the counterstain. All steps were performed at room temperature unless otherwise noted. HMGA2 protein expression (brown) versus background (blue) staining was evaluated using a semi-automated image analysis system (ACISII, Chromavision) (71), and the results of two separate sections from

each sample were averaged. HMGA2 staining for each t(12;14) UL sample is expressed as a fold change compared with a matched non-t(12;14) UL from the same patient.

Immunohistochemistry for CCND1

Immunohistochemistry to detect CCND1 protein in t(12;14) UL and matched non-t(12;14) UL for Cases 4 and 5 was performed in the Specialized Histology Core of the Dana-Farber/Harvard Cancer Center. Five-micron formalin-fixed, paraffin-embedded tissue sections were deparaffinized and subjected to antigen retrieval in a pressure cooker for 2 min in citrate buffer. After washing, the endogenous peroxidase activity was quenched (Peroxidase block, Dako) for 20 min and slides were incubated with rabbit polyclonal anti-cyclin D1 antibody (1:40, Thermo Fisher Scientific) for 60 min. Following washing, the Envision Plus detection system (Dako) was applied, including a 30 min incubation with goat anti-rabbit immunoglobulin conjugated to a peroxidase-labeled polymer (HRP) followed by a 5 min exposure to the substrate diaminobenzidine (DAB) to produce a brown precipitate visible by microscopy. Hematoxylin was used as the counterstain. All steps subsequent to antigen retrieval were performed at room temperature. CCND1 protein expression (brown) versus background (blue) staining was evaluated by dividing each stained tumor into four quadrants, visually assessing 20 nuclei in each quadrant and then averaging the data from the four quadrants. The results of two separate sections from each tumor were also averaged. CCND1 staining for each t(12;14) UL sample is expressed as fold change compared with a non-t(12;14) UL from the same patient.

RNA isolation

A portion of each of the myometrial, non-t(12;14) UL and t(12;14) UL tissues was frozen in liquid nitrogen immediately after surgical removal or placed directly into RNAlater solution (QIAGEN). RNA was isolated using the RNeasy Fibrous Tissue kit with a provided standard protocol (QIAGEN) and assessed for purity and quantity on a Nanodrop spectrophotometer (Thermo Scientific).

Q-PCR for *HMGA2*

Quantitative PCR was performed as previously described (14) using the standard curve method and normalizing the level of *HMGA2* in each tissue to that of *GAPDH*.

Q-PCR for *CCND1* and *CCND2*

Total RNA from the t(12;14) and non-t(12;14) UL from each of five women (Cases 1, 4, 6, 8 and 9) was examined for *CCND1* and *CCND2* gene expression. PCR was performed on the ABI PRISM 7900HT Sequence Detection System in a 384-well format. TaqMan Universal PCR MasterMix and a pre-designed and optimized Taqman Gene Expression Assay for quantitation of human *CCND1* or *CCND2* RNA (Applied Biosystems) were used according to the manufacturer's instructions. Each RNA was run in quadruplicate and the C_t (cycle threshold) values of these replicates were averaged

and then normalized by subtracting the C_t value of the co-amplified internal control housekeeping gene *GAPDH* for a ΔC_t value. Data analysis used the comparative C_t method where the ΔC_t of a non-t(12;14) UL was used as a calibrator reference and subtracted from the ΔC_t of the corresponding t(12;14) UL to yield a $\Delta\Delta C_t$ value. This was then converted into a fold-change relative to one using the following formula: *CCND1* or *CCND2* expression $= 2^{(-\Delta\Delta C_t)}$. For each gene, this number was then averaged across the five samples.

Transcriptional profiling

Total RNA isolated from the myometrial, non-t(12;14) UL and t(12;14) UL tissues from each of nine cases was assessed for quality by RNA Nano LabChip analysis on an Agilent Bioanalyzer 2100 and then applied to GeneChip Human Genome U133 Plus 2.0 oligonucleotide expression microarrays (Affymetrix). Standard protocols as described in the Affymetrix GeneChip Expression Analysis Technical Manual revision 5 were employed at the Harvard Medical School—Partners HealthCare Center for Genetics and Genomics (HPCGG). Briefly, 5 µg of total RNA template from each sample was reverse-transcribed into cDNA using oligo-dT primer containing T7 RNA polymerase-binding sites using the GeneChip Expression 3′-Amplification Reagents One-Cycle cDNA Synthesis kit with subsequent purification of the double-stranded product with Affymetrix GeneChip Cleanup Module (Affymetrix). *In vitro* transcription to produce complementary RNA (cRNA) using T7 Polymerase and biotinylated dUTP and dCTP was performed with the GeneChip Expression Amplification Reagents kit (Affymetrix) and the biotin-labeled product quantitated on a UV plate reader (Bio-Tek). Following purification and fragmentation to reduce secondary structure, hybridization occurred overnight at 45°C in a Model 640 hybridization chamber to expression microarrays containing over 54 000 oligonucleotide probe sets representing more than 47 000 transcripts and 38 500 well-characterized genes. Arrays were washed using a Model 450 Fluidics station with GeneChip Operating Software (Affymetrix) and then scanned by the GeneChip Model 3000 7G. Array images were inspected visually for experimental artifacts and various quality measurements such as present versus absent calls and RNA degradation were examined to verify the quality of the data. Probe set expression values were calculated by GeneChip software using the MAS 5.0 algorithm. Probe sets with fewer than five present calls among the t(12;14), non-t(12;14) and myometrium arrays were excluded. Paired differential expression analysis (not accounting for percent mosaicism) between t(12;14) and non-t(12;14) UL was computed using paired *t*-tests in which tissue samples were analyzed as matched pairs based on patient status. Mosaicism-weighted paired differential expression analysis was implemented in the Bioconductor (72) package *limma* (73) by fitting a linear model with weights equal to the percent mosaicism. All differential expression analyses were corrected for multiple testing using the false discovery rate (*Q*-value). Data analysis was carried out in the statistical language R (http://www.r-project.org).

Expression data were deposited at the NCBI Gene Expression Omnibus (GEO; http://www.ncbi.nlm.nih.gov/geo/); the series entry number is GSE18096 and the specific accession identifiers are listed in Table 1.

Ingenuity Pathways Analysis and Gene Set Enrichment Analysis

Functional analysis of the 374 probe sets with a *P*-value of ≤0.005 from the t(12;14) UL-specific gene list weighted for t(12;14) cell mosaicism was performed using IPA (Ingenuity Systems, www.Ingenuity.com). Networks were generated to look for interactions of the t(12;14) UL-specific genes with others based on the literature as curated in the Ingenuity Pathway Knowledge Base. Fisher's exact test was used to calculate statistical significance of a network, which is the probability of observing the number of genes from the t(12;14) UL-specific gene list given the number of genes belonging to the network. The network score is calculated by $-\log_{10}$ (*P*-value). Networks with a score of 8–46 were highly significant and included 7–25 genes from the t(12;14) UL-specific list.

For the GSEA method, 700 gene ontology (GO) functional annotations that have ≥20 genes and ≤500 genes were collected from MSigDB (http://www.broadinstitute.org/gsea/msigdb/index.jsp; MSigDB c5 GO category). The extent of enrichment (enrichment score) was calculated for the individual GO categories using the weighted Kolmogorov–Smirnov statistic as described previously (34). The significance was determined based on 1000 gene permutation tests and adjusted for multiple tests.

Analysis of merged del(7q) UL and t(12;14) UL data sets

The t(12;14) UL expression data and the published del(7q) UL data (GEO accession GSE12814) (32), which used the same array platform (GeneChip Human Genome U133 Plus 2.0), were merged. The combined expression profile was processed using ComBat (35) to adjust for batch effect. Agglomerative hierarchical clustering was performed on the 1000 top variable genes using Pearson's correlation as distance with average linkage. To test the hypothesis that myometrium from t(12;14) versus del(7q) patients can be distinguished based on expression profiles, the *k*-NN method was employed (74). In leave-one-out cross-validation tests for 16 predictions of seven t(12;14) and nine del(7q) myometrium, the prediction accuracy of 100% was achieved with a class predictor size of 20 genes. We report nine genes (*PLP1*, *MEST*, *PCDH20*, *SLC26A7*, *BCL11A*, *PRL*, *LOC727770*, *CAPN6* and *PLAG1*) that were observed in all 16 sets of class predictors.

SUPPLEMENTARY MATERIAL

Supplementary Material is available at *HMG* online.

ACKNOWLEDGEMENTS

REFERENCES

1. Cramer, S.F. and Patel, A. (1990) The frequency of uterine leiomyomas. *Am. J. Clin. Pathol.*, **94**, 435–438.
2. Coronado, G.D., Marshall, L.M. and Schwartz, S.M. (2000) Complications in pregnancy, labor, and delivery with uterine leiomyomas: a population-based study. *Obstet. Gynecol.*, **95**, 764–769.
3. Buttram, V.C. Jr and Reiter, R.C. (1981) Uterine leiomyomata: etiology, symptomatology, and management. *Fertil. Steril.*, **36**, 433–445.
4. Viswanathan, M., Hartmann, K., McKoy, N., Stuart, G., Rankins, N., Thieda, P., Lux, L.J. and Lohr, K.N. (2007) Management of uterine fibroids: an update of the evidence. *Evid. Rep. Technol. Assess. (Full Rep)*, **154**, 1–122.
5. Flynn, M., Jamison, M., Datta, S. and Myers, E. (2006) Health care resource use for uterine fibroid tumors in the United States. *Am. J. Obstet. Gynecol.*, **195**, 955–964.
6. Hartmann, K.E., Birnbaum, H., Ben-Hamadi, R., Wu, E.Q., Farrell, M.H., Spalding, J. and Stang, P. (2006) Annual costs associated with diagnosis of uterine leiomyomata. *Obstet. Gynecol.*, **108**, 930–937.
7. Lepine, L.A., Hillis, S.D., Marchbanks, P.A., Koonin, L.M., Morrow, B., Kieke, B.A. and Wilcox, L.S. (1997) Hysterectomy surveillance—United States, 1980–1993. *MMWR CDC Surveill. Summ.*, **46**, 1–15.
8. Nilbert, M. and Heim, S. (1990) Uterine leiomyoma cytogenetics. *Genes Chrom. Cancer*, **2**, 3–13.
9. Rein, M.S., Friedman, A.J., Barbieri, R.L., Pavelka, K., Fletcher, J.A. and Morton, C.C. (1991) Cytogenetic abnormalities in uterine leiomyomata. *Obstet. Gynecol.*, **77**, 923–926.
10. Meloni, A.M., Surti, U., Contento, A.M., Davare, J. and Sandberg, A.A. (1992) Uterine leiomyomas: cytogenetic and histologic profile. *Obstet. Gynecol.*, **80**, 209–217.
11. Hennig, Y., Deichert, U., Bonk, U., Thode, B., Bartnitzke, S. and Bullerdiek, J. (1999) Chromosomal translocations affecting 12q14–15 but not deletions of the long arm of chromosome 7 associated with a growth advantage of uterine smooth muscle cells. *Mol. Hum. Reprod.*, **5**, 1150–1154.
12. Brosens, I., Deprest, J., Dal Cin, P. and Van den Berghe, H. (1998) Clinical significance of cytogenetic abnormalities in uterine myomas. *Fertil. Steril.*, **69**, 232–235.
13. Rein, M.S., Powell, W.L., Walters, F.C., Weremowicz, S., Cantor, R.M., Barbieri, R.L. and Morton, C.C. (1998) Cytogenetic abnormalities in uterine myomas are associated with myoma size. *Mol. Human Repro.*, **4**, 83–86.
14. Gross, K.L., Neskey, D.M., Manchanda, N., Weremowicz, S., Kleinman, M.S., Nowak, R.A., Ligon, A.H., Rogalla, P., Drechsler, K., Bullerdiek, J. *et al.* (2003) HMGA2 expression in uterine leiomyomata and myometrium: quantitative analysis and tissue culture studies. *Genes Chrom. Cancer*, **38**, 68–79.
15. Gattas, G.J., Quade, B.J., Nowak, R.A. and Morton, C.C. (1999) HMGIC expression in human adult and fetal tissues and in uterine leiomyomata. *Genes Chrom. Cancer*, **25**, 316–322.
16. Wolffe, A.P. (1994) Architectural transcription factors. *Science*, **264**, 1100–1101.
17. Reeves, R. (2001) Molecular biology of HMGA proteins: hubs of nuclear function. *Gene*, **277**, 63–81.
18. Ashar, H.R., Cherath, L., Przybysz, K.M. and Chada, K. (1996) Genomic characterization of human HMGIC, a member of the accessory transcription factor family found at translocation breakpoints in lipomas. *Genomics*, **31**, 207–214.
19. Grosschedl, R., Giese, K. and Pagel, J. (1994) HMG domain proteins: architectural elements in the assembly of nucleoprotein structures. *Trends Genet.*, **10**, 94–100.
20. Hirning-Folz, U., Wilda, M., Rippe, V., Bullerdiek, J. and Hameister, H. (1998) The expression pattern of the Hmgic gene during development. *Genes Chrom. Cancer*, **23**, 350–357.
21. Zhou, X., Benson, K.F., Ashar, H.R. and Chada, K. (1995) Mutation responsible for the mouse pygmy phenotype in the developmentally regulated factor HMGI-C. *Nature*, **376**, 771–774.
22. Rogalla, P., Drechsler, K., Frey, G., Hennig, Y., Helmke, B., Bonk, U. and Bullerdiek, J. (1996) HMGI-C expression patterns in human tissues. Implications for the genesis of frequent mesenchymal tumors. *Am. J. Pathol.*, **149**, 775–779.
23. Zhou, X., Benson, K.F., Przybysz, K., Liu, J., Hou, Y., Cherath, L. and Chada, K. (1996) Genomic structure and expression of the murine Hmgi-c gene. *Nucleic Acids Res.*, **24**, 4071–4077.
24. Nissen, M.S., Langan, T.A. and Reeves, R. (1991) Phosphorylation by cdc2 kinase modulates DNA binding activity of high mobility group I nonhistone chromatin protein. *J. Biol. Chem.*, **266**, 19945–19952.
25. Hodge, J.C., T Cuenco,, K., Huyck, K.L., Somasundaram, P., Panhuysen, C.I., Stewart, E.A. and Morton, C.C. (2009) Uterine leiomyomata and decreased height: a common HMGA2 predisposition allele. *Hum. Genet.*, **125**, 257–263.
26. Weedon, M.N., Lettre, G., Freathy, R.M., Lindgren, C.M., Voight, B.F., Perry, J.R., Elliott, K.S., Hackett, R., Guiducci, C., Shields, B. *et al.* (2007) A common variant of HMGA2 is associated with adult and childhood height in the general population. *Nat. Genet.*, **39**, 1245–1250.
27. Ligon, A.H., Moore, S.D., Parisi, M.A., Mealiffe, M.E., Harris, D.J., Ferguson, H.L., Quade, B.J. and Morton, C.C. (2005) Constitutional rearrangement of the architectural factor HMGA2: a novel human phenotype including overgrowth and lipomas. *Am. J. Hum. Genet.*, **76**, 340–348.
28. Berthois, Y., Katzenellenbogen, J.A. and Katzenellenbogen, B.S. (1986) Phenol red in tissue culture media is a weak estrogen: implications concerning the study of estrogen-responsive cells in culture. *Proc. Natl Acad. Sci. USA*, **83**, 2496–2500.
29. Hashimoto, K., Azuma, C., Kamiura, S., Kimura, T., Nobunaga, T., Kanai, T., Sawada, M., Noguchi, S. and Saji, F. (1995) Clonal determination of uterine leiomyomas by analyzing differential inactivation of the X-chromosome-linked phosphoglycerokinase gene. *Gynecol. Obstet. Invest.*, **40**, 204–208.
30. Linder, D. and Gartler, S.M. (1965) Glucose-6-phosphate dehydrogenase mosaicism: utilization as a cell marker in the study of leiomyomas. *Science*, **150**, 67–69.
31. Mashal, R.D., Fejzo, M.L., Friedman, A.J., Mitchner, N., Nowak, R.A., Rein, M.S., Morton, C.C. and Sklar, J. (1994) Analysis of androgen receptor DNA reveals the independent clonal origins of uterine leiomyomata and the secondary nature of cytogenetic aberrations in the development of leiomyomata. *Genes Chrom. Cancer*, **11**, 1–6.
32. Hodge, J.C., Park, P.J., Dreyfuss, J.M., Assil-Kishawi, I., Somasundaram, P., Semere, L.G., Quade, B.J., Lynch, A.M., Stewart, E.A. and Morton, C.C. (2009) Identifying the molecular signature of the interstitial deletion 7q subgroup of uterine leiomyomata using a paired analysis. *Genes Chrom. Cancer*, **48**, 865–885.
33. Storey, J.D. and Tibshirani, R. (2003) Statistical significance for genomewide studies. *Proc. Natl Acad. Sci. USA*, **100**, 9440–9445.
34. Subramanian, A., Tamayo, P., Mootha, V.K., Mukherjee, S., Ebert, B.L., Gillette, M.A., Paulovich, A., Pomeroy, S.L., Golub, T.R., Lander, E.S. *et al.* (2005) Gene set enrichment analysis: a knowledge-based approach for interpreting genome-wide expression profiles. *Proc. Natl Acad. Sci. USA*, **102**, 15545–15550.
35. Johnson, W.E., Li, C. and Rabinovic, A. (2007) Adjusting batch effects in microarray expression data using empirical Bayes methods. *Biostatistics*, **8**, 118–127.
36. Fusco, A. and Fedele, M. (2007) Roles of HMGA proteins in cancer. *Nat. Rev. Cancer*, **7**, 899–910.
37. Schoenmakers, E.F., Wanschura, S., Mols, R., Bullerdiek, J., Van den Berghe, H. and Van de Ven, W.J. (1995) Recurrent rearrangements in the

high mobility group protein gene, HMGI-C, in benign mesenchymal tumours. *Nat. Genet.*, **10**, 436–444.

38. Berner, J.M., Meza-Zepeda, L.A., Kools, P.F., Forus, A., Schoenmakers, E.F., Van de Ven, W.J., Fodstad, O. and Myklebost, O. (1997) HMGIC, the gene for an architectural transcription factor, is amplified and rearranged in a subset of human sarcomas. *Oncogene*, **14**, 2935–2941.

39. Cha, P.C., Takahashi, A., Hosono, N., Low, S.K., Kamatani, N., Kubo, M. and Nakamura, Y. (2011) A genome-wide association study identifies three loci associated with susceptibility to uterine fibroids. *Nat. Genet.*, **43**, 447–450.

40. Geurts, J.M., Schoenmakers, E.F., Roijer, E., Astrom, A.K., Stenman, G. and van de Ven, W.J. (1998) Identification of NFIB as recurrent translocation partner gene of HMGIC in pleomorphic adenomas. *Oncogene*, **16**, 865–872.

41. Hensen, K., Braem, C., Declercq, J., Van Dyck, F., Dewerchin, M., Fiette, L., Denef, C. and Van de Ven, W.J. (2004) Targeted disruption of the murine Plag1 proto-oncogene causes growth retardation and reduced fertility. *Dev. Growth Differ.*, **46**, 459–470.

42. Hensen, K., Van Valckenborgh, I.C., Kas, K., Van de Ven, W.J. and Voz, M.L. (2002) The tumorigenic diversity of the three PLAG family members is associated with different DNA binding capacities. *Cancer Res.*, **62**, 1510–1517.

43. Voz, M.L., Mathys, J., Hensen, K., Pendeville, H., Van Valckenborgh, I., Van Huffel, C., Chavez, M., Van Damme, B., De Moor, B., Moreau, Y. *et al.* (2004) Microarray screening for target genes of the proto-oncogene PLAG1. *Oncogene*, **23**, 179–191.

44. Landrette, S.F., Kuo, Y.H., Hensen, K., Barjesteh van Waalwijk van Doorn-Khosrovani, S., Perrat, P.N., Van de Ven, W.J., Delwel, R. and Castilla, L.H. (2005) Plag1 and Plagl2 are oncogenes that induce acute myeloid leukemia in cooperation with Cbfb-MYH11. *Blood*, **105**, 2900–2907.

45. Nohara, A., Ohmichi, M., Koike, K., Jikihara, H., Kimura, A., Masuhara, K., Ikegami, H., Inoue, M., Miyake, A. and Murata, Y. (1997) Prolactin stimulates mitogen-activated protein kinase in human leiomyoma cells. *Biochem. Biophys. Res.Commun.*, **238**, 473–477.

46. Nowak, R.A., Mora, S., Diehl, T., Rhoades, A.R. and Stewart, E.A. (1999) Prolactin is an autocrine or paracrine growth factor for human myometrial and leiomyoma cells. *Gynecol. Obstet. Invest.*, **48**, 127–132.

47. Arslan, A.A., Gold, L.I., Mittal, K., Suen, T.C., Belitskaya-Levy, I., Tang, M.S. and Toniolo, P. (2005) Gene expression studies provide clues to the pathogenesis of uterine leiomyoma: new evidence and a systematic review. *Hum. Reprod.*, **20**, 852–863.

48. Lefebvre, L., Viville, S., Barton, S.C., Ishino, F., Keverne, E.B. and Surani, M.A. (1998) Abnormal maternal behaviour and growth retardation associated with loss of the imprinted gene Mest. *Nat. Genet.*, **20**, 163–169.

49. Skubitz, K.M. and Skubitz, A.P. (2003) Differential gene expression in uterine leiomyoma. *J. Lab. Clin. Med.*, **141**, 297–308.

50. Rho, S.B., Byun, H.J., Park, S.Y. and Chun, T. (2008) Calpain 6 supports tumorigenesis by inhibiting apoptosis and facilitating angiogenesis. *Cancer Lett.*, **271**, 306–313.

51. Satterwhite, E., Sonoki, T., Willis, T.G., Harder, L., Nowak, R., Arriola, E.L., Liu, H., Price, H.P., Gesk, S., Steinemann, D. *et al.* (2001) The BCL11 gene family: involvement of BCL11A in lymphoid malignancies. *Blood*, **98**, 3413–3420.

52. Grossel, M.J., Baker, G.L. and Hinds, P.W. (1999) cdk6 can shorten G(1) phase dependent upon the N-terminal INK4 interaction domain. *J. Biol. Chem.*, **274**, 29960–29967.

53. Resnitzky, D., Gossen, M., Bujard, H. and Reed, S.I. (1994) Acceleration of the G1/S phase transition by expression of cyclins D1 and E with an inducible system. *Mol. Cell. Biol.*, **14**, 1669–1679.

54. Timmermann, S., Hinds, P.W. and Munger, K. (1997) Elevated activity of cyclin-dependent kinase 6 in human squamous cell carcinoma lines. *Cell Growth Differ.*, **8**, 361–370.

55. Donnellan, R. and Chetty, R. (1998) Cyclin D1 and human neoplasia. *Mol. Pathol.*, **51**, 1–7.

56. Easton, J., Wei, T., Lahti, J.M. and Kidd, V.J. (1998) Disruption of the cyclin D/cyclin-dependent kinase/INK4/retinoblastoma protein regulatory pathway in human neuroblastoma. *Cancer Res.*, **58**, 2624–2632.

57. Costello, J.F., Plass, C., Arap, W., Chapman, V.M., Held, W.A., Berger, M.S., Su Huang, H.J. and Cavenee, W.K. (1997) Cyclin-dependent kinase 6 (CDK6) amplification in human gliomas identified using two-dimensional separation of genomic DNA. *Cancer Res.*, **57**, 1250–1254.

58. Lanahan, A., Williams, J.B., Sanders, L.K. and Nathans, D. (1992) Growth factor-induced delayed early response genes. *Mol. Cell. Biol.*, **12**, 3919–3929.

59. Tavtigian, S.V., Zabludoff, S.D. and Wold, B.J. (1994) Cloning of mid-G1 serum response genes and identification of a subset regulated by conditional myc expression. *Mol. Biol. Cell*, **5**, 375–388.

60. Li, D., Lin, H.H., McMahon, M., Ma, H. and Ann, D.K. (1997) Oncogenic raf-1 induces the expression of non-histone chromosomal architectural protein HMGI-C via a p44/p42 mitogen-activated protein kinase-dependent pathway in salivary epithelial cells. *J. Biol. Chem.*, **272**, 25062–25070.

61. Ayoubi, T.A., Jansen, E., Meulemans, S.M. and Van de Ven, W.J. (1999) Regulation of HMGIC expression: an architectural transcription factor involved in growth control and development. *Oncogene*, **18**, 5076–5087.

62. Brants, J.R., Ayoubi, T.A., Chada, K., Marchal, K., Van de Ven, W.J. and Petit, M.M. (2004) Differential regulation of the insulin-like growth factor II mRNA-binding protein genes by architectural transcription factor HMGA2. *FEBS Lett.*, **569**, 277–283.

63. Cleynen, I., Brants, J.R., Peeters, K., Deckers, R., Debiec-Rychter, M., Sciot, R., Van de Ven, W.J. and Petit, M.M. (2007) HMGA2 regulates transcription of the Imp2 gene via an intronic regulatory element in cooperation with nuclear factor-kappaB. *Mol. Cancer Res.*, **5**, 363–372.

64. Nielsen, J., Christiansen, J., Lykke-Andersen, J., Johnsen, A.H., Wewer, U.M. and Nielsen, F.C. (1999) A family of insulin-like growth factor II mRNA-binding proteins represses translation in late development. *Mol. Cell. Biol.*, **19**, 1262–1270.

65. Stewart, E.A. and Nowak, R.A. (1998) New concepts in the treatment of uterine leiomyomas. *Obstet. Gynecol.*, **92**, 624–627.

66. Semenza, G.L. (2003) Targeting HIF-1 for cancer therapy. *Nat. Rev. Cancer*, **3**, 721–732.

67. Forristal, C.E., Wright, K.L., Hanley, N.A., Oreffo, R.O. and Houghton, F.D. (2010) Hypoxia inducible factors regulate pluripotency and proliferation in human embryonic stem cells cultured at reduced oxygen tensions. *Reproduction*, **139**, 85–97.

68. Cheung, V.G., Nowak, N., Jang, W., Kirsch, I.R., Zhao, S., Chen, X.N., Furey, T.S., Kim, U.J., Kuo, W.L., Olivier, M. *et al.* (2001) Integration of cytogenetic landmarks into the draft sequence of the human genome. *Nature*, **409**, 953–958.

69. Karolchik, D., Baertsch, R., Diekhans, M., Furey, T.S., Hinrichs, A., Lu, Y.T., Roskin, K.M., Schwartz, M., Sugnet, C.W., Thomas, D.J. *et al.* (2003) The UCSC Genome Browser Database. *Nucleic Acids Res.*, **31**, 51–54.

70. Moore, S.D., Herrick, S.R., Ince, T.A., Kleinman, M.S., Cin, P.D., Morton, C.C. and Quade, B.J. (2004) Uterine leiomyomata with t(10;17) disrupt the histone acetyltransferase MORF. *Cancer Res.*, **64**, 5570–5577.

71. Bismar, T.A., Demichelis, F., Riva, A., Kim, R., Varambally, S., He, L., Kutok, J., Aster, J.C., Tang, J., Kuefer, R. *et al.* (2006) Defining aggressive prostate cancer using a 12-gene model. *Neoplasia*, **8**, 59–68.

72. Gentleman, R.C., Carey, V.J., Bates, D.M., Bolstad, B., Dettling, M., Dudoit, S., Ellis, B., Gautier, L., Ge, Y., Gentry, J. *et al.* (2004) Bioconductor: open software development for computational biology and bioinformatics. *Genome Biol.*, **5**, R80.

73. Smyth, G.K. (2004) Linear models and empirical Bayes methods for assessing differential expression in microarray experiments. *Stat. Appl. Genet. Mol. Biol.*, **3**, Article3.

74. Golub, T.R., Slonim, D.K., Tamayo, P., Huard, C., Gaasenbeek, M., Mesirov, J.P., Coller, H., Loh, M.L., Downing, J.R., Caligiuri, M.A. *et al.* (1999) Molecular classification of cancer: class discovery and class prediction by gene expression monitoring. *Science*, **286**, 531–537.